Vibration Spectrum Analysis for Cryogenic Gravitational Wave Detectors

V. Tempesta[1, a)]
Physics dept., Moravian College

(Dated: August 2, 2017)

Silicon suspensions are currently an attractive solution for providing low thermal noise mirror suspensions for gravitational wave detectors at cryogenic temperatures. The Institute for Gravitational Research (IGR) at the University of Glasgow is currently developing a small scale prototype with a test mass of a few kg, suspended initially from ribbon fibres, but ultimately utilizing circular cross section fibres grown via the Laser Heated Pedestal Growth technique. This article reports on summer work carried out by the author within the IGR researching aspects of the design and fabrication of the silicon suspension, which will be housed in a cryogen-free cryocooler. This project includes some analysis of the optimum suspension geometry, and tests in the cryocooled system including measuring the vibration spectrum and cooling time of silicon ribbon geometries. Overall, it was found that the system is vibrating consistently at 7 Hz all over and oscillates horizontally at 4 and 10 Hz as well near the base of the external frame. To combat this it is proposed to add damping mechanisms such as stabilizing beams to lower the overall thermal noise of the system.

Keywords: Gravitational physics, Cryocooler, gravitational waves, silicon, MEMS

During this project I measured the vibration spectra of multiple points on a pulse cooled cryostat. Using this information, I determined possible damping solutions to isolate the test masses from external vibrations. I will first introduce the field of gravitational waves and some background for this project at the University of Glasgow.

I. INTRODUCTION

In 1914, Einstein predicted the existence of gravitational waves through his Theory of General Relativity. [15] In his theory, he showed that gravity wasn,t a physical force, but instead a bend in the fabric of space-time. This can be thought of as a bowling ball sitting on a trampoline. As the bowling ball sits there in the fabric of space-time, the trampoline is warped and this warping affects the objects around it. The more massive an object, the greater disturbance it will cause in the fabric. If the Sun were the bowling ball then the Earth would be a marble rolling along the natural curvature of space, spiraling around the Sun and thus creating an elliptical orbit. This is how Einstein represented gravity between two objects in space.

Einstein predicted that if two large masses fell into each other's gravitational pull, they would begin to orbit around each other at such high speeds that the warps in space-time that they created would ripple outward at the speed of light. These ripples in space-time are called **gravitational waves**. Key characteristics of gravitational waves are that they travel at the speed of light, have two independent polarizations and are characterized by an amplitude that is conventionally called h, which is twice the strain induced in a system of free particles by the gravitational wave. [1]

On September 14th, 2015, Einstein,s hundred year old predictions were verified. For the first time in history, a gravitational wave was physically detected. [16] This was huge news for the community and for humanity as a whole. These detections can tell us so much about the universe around us. They allow us to obtain more information on topics such as the mechanisms of stellar collapse, the expansion of the universe, the equation of state of neutron star material, and the nature of gravity itself.

Gravitational waves are formed whenever mass moves asymmetrically. However, only the biggest gravitational waves that cause the most significant disturbances in space-time can be detected. These massive waves are produced by catastrophic events in the far distant universe such as colliding black holes, the collapse of stellar cores (supernovae), coalescing compact binary systems of neutron stars or white dwarf stars, the slightly wobbly rotation of neutron stars that are not perfect spheres (pulsars), and the remnants of gravitational radiation created by the birth of the Universe itself. [2]

From the 1960's to the 1980's the idea of using interferometers as gravitational wave detectors was developed and in the 1990's several ground based detectors were built, starting with the Laser Interferometer Gravitational-Wave Observatory (LIGO) in the USA and GEO600 in Germany who both started collecting data in 2002, soon followed by Virgo in Italy starting up in 2007. In 2015, the first gravitational wave signal was detected at LIGO. [11] This was notably one of the greatest scientific discoveries of all time. So how did they do it?

A. Gravitational wave detectors

The answer is Michelson Interferometry. The Michelson interferometer was invented by American Physicist

a)Electronic mail: stpft01@moravian.edu

Albert A. Michelson in 1887. He and his colleague Dr. Edward Morley developed this experiment for the purpose of finding out if the Ether existed by measuring it against the Earth's velocity. [17] His experiment proved that Earth did not in fact move relative to Ether and his findings then worked to inspire Einstein's General Theory of Relativity. We now use interferometers to detect the gravitational waves that Einstein then predicted in his theory.

The system consists of mirrors and semi-transparent mirrors (or beamsplitters) for merging separated beams of light, which are coming from the same source. They are called interferometers because they work by merging two or more sources of light to create an interference pattern. These interference patterns tells us about the environment that the lasers are moving through such as the refractive index of the medium it's traveling through. Interferometers are great for detecting small measurements that can't be measured any other way. To measure a gravitational wave, one needs to be able to detect distance changes of at least 10^{-18} meters, which is equivalent to 1/10,000 the width of a proton.

It works by sending a singular beam of light through a beamsplitter at which some of the light is reflected off and some travels through the mirror. There are now two identical beams of light traveling perpendicular to each other. These beams of light travel down four kilometers of evacuated tube until they reach a fused silica test mass that reflects the beam back. The beam bounces back and forth in the long tube until it recombines with its other half at the beamsplitter and travels down a new path to a photodetector. This detector sees the two beams of light and determines if they are constructively or destructively interfering with each other. When a gravitational wave passes, it warps space-time as it moves through the detector. As a result, one arm of the detector will be stretched or contracted in comparison to the other arm. If there is no gravitational wave present, when the two beams of light recombine, the beams will have both traveled the same distance and will arrive perfectly in sync with one another when they recombine. The photodetector will see this as a singular constant beam of light. If there is a gravitational wave that passes through, one beam will have to travel a longer distance than its other half and when they recombine, they will be at different positions and the two waves will destructively or constructively interfere with one another and will produce a detectable interference pattern.

At the University of Glasgow, there is a Fabry-Perot based prototype detector of 10 m arm length that has been in operation since 1978 but has been operating in it's phase 2 upgrade since 2002. [12] To achieve the interferometer's required long path length in the arms, the University of Glasgow uses the Fabry-Perot technique. This Fabry-Perot scheme was developed at Glasgow and Caltech. What makes this scheme unique is that it requires much smaller mirrors and the light beams occupy a much smaller volume in the interferometer arms. This detector has a GEO-like infrastructure with similar vacuum systems, triple Stage GEO-suspensions, and the same local control system.

As Hough et. al. states in their proposal, "For optical path length changes small compared with the wavelength of the gravitational wave (300 km for a 1 kHz signal) the phase shift is proportional to the length of each arm. Thus, one can gain in sensitivity both by increasing the physical arm-length of the interferometer, and by bouncing the light back and forth many times in each arm before interference takes place at the beamsplitter." [1] There are many things we can do to improve the sensitivity of these detectors. For example, LIGO has now initiated the Advanced LIGO phase. Initial LIGO's suspension was a single pendulum design with an 11 kg test mass hung by steel fibers. Advanced LIGO's suspension system is a *much* heftier quadruple pendulum with a 40 kg test mass hung by four fused silica fibers. Advanced LIGO also incorporates an active seismic isolation system as well as a passive one. This additional system monitors any slight changes in movement of hundreds of LIGO components and immediately counteracts these detected movements using feedback. These improvements were designed to further reduce the vibrations reaching the interferometers' mirrors: unwanted vibrations that could drown out the exceedingly small signals from a gravitational wave. [4]

Virgo in Italy has also made substantial improvements to its initial design and is now in its Advanced Virgo stages. Preparations for a space-based gravitational wave detector, LISA, standing for Laser Interferometer Space Antenna, have started. LISA will consist of three spacecraft that are separated by millions of miles and trailing behind the Earth as we orbit the Sun. These three spacecraft relay lasers back and forth between them. The LISA detector footprint as a whole is much bigger than the size of the Earth. This allows us to observe lower frequency gravitational wave signals that cannot be detected by ground-based interferometers.

To maximize the potential of the Glasgow 10m detector, the IGR carries out several strands of experiments in parallel. They conduct direct measurement of thermal noise in the green portion of Figure 2. Using a 3-mirror coupled cavity systems (see the blue section of Figure 2), they conduct experiments on control strategies, radiation pressure, and frequency references for thermal noise experiments. In the red diffractive interferometry portion of Figure 2, they do experiments on using grating as cavity incoupler and they plan to do and experiment on using a waveguide mirror in a suspended cavity. [12]

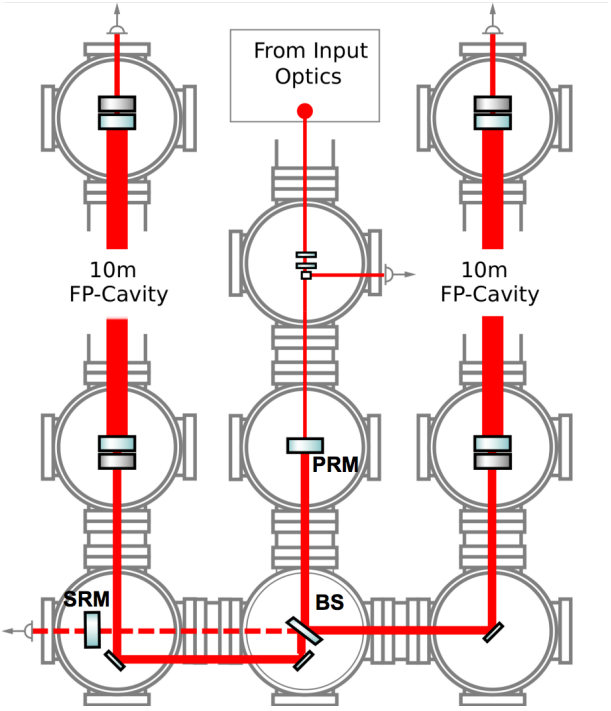

Figure 1: Schematic of 10m Glasgow Detector [12]

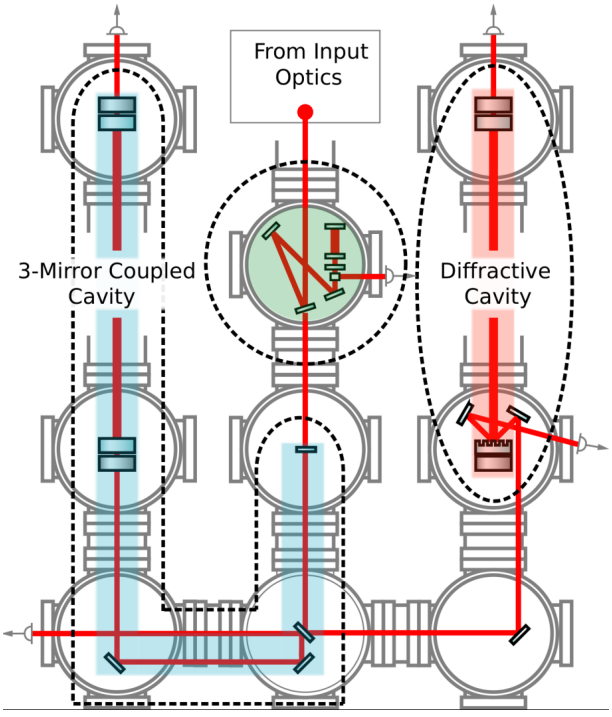

Figure 2: Schematic of 10m Glasgow Detector [12]

B. Noise sources in gravitational wave detectors

The limiting factor to the detector's sensitivity is noise. There are many kinds of noise that can affect the system. In this article, thermal noise is mainly be investigated but we will first go over some of the many other sources.

One source of noise is **optical noise**. Optical noise consists of shot noise and quantum noise and is defined as false phase fluctuations caused by fluctuations in the frequency, power and geometry of the light. This could be due to possible coupling via scattered light. **Shot noise** is a problem that must be accounted for in these systems. The photons in a laser beam are not equally distributed in time but instead follow a Poisson distribution. This means that any laser beam detected by a photodiode will cause the output of the photodiode to carry noise. Shot noise is the noise that comes from the amount of photons hitting the mirror. "This shot noise, which scales proportional to the square root of the detected optical power, can be considered as the readout or sensing noise of the interferometer." [5] Another concern is **seismic noise**. This comes from ground vibrations and threatens to move the test masses. There are many isolation measures that are in place to reduce this such as having a multi-pendulum system but is only effective around 10 Hz.

The main noise source is **thermal noise**. Thermal noise consists of thermoelastic noise and Brownian noise. The thermal noise in the suspensions comes from mechanical dissipation in the materials that make up the suspension (Brownian noise) or through the coupling of statistical temperature fluctuations through the thermomechanical properties of the suspension materials (Thermoelastic noise). [8] The noise source that I will be investigating in this project is the **thermoelastic noise**. This is due to dissipative heat flux as the sample bends while being excited. Most current gravitational wave detectors use fused silica as the test mass and suspension material. However, at lower temperatures (around 40 K) these fused silica test masses begin to oscillate and there is higher levels of dissipation. During this oscillation, some parts of the material are heated and some are cooled, depending on which way the sample is bending. This is thermoelastic noise. The difference in temperature causes a heat flux which results in something called *dissipation*. This high level of dissipation from the fused silica causes it not to be a usable test mass at these lower temperatures because of the increased thermal noise due to the dissipation.

C. Next generation detectors

Currently next generation detectors are being developed across the world. For example, the KAGRA project in Japan and the Einstein Telescope (ET) in Europe. Current gravitational wave detectors operate at room temperature and are ground-based. However, in the fu-

ture, these next generation detectors will operate at cryogenic temperatures and underground. This will work to eliminate or minimize many noise sources such as seismic noise.

KAGRA was previously known as LCGT, Large-scale Cryogenic Gravitational-wave Telescope and is a Japanese interferometer in the Kamioka mine. It is currently under construction. Due to the detector being underground, KAGRA reduces Newtonian noise and it also reduces the thermal noise that the system feels by operating at cryogenic temperatures around 20 K. At around 40 K, the fused silica test masses and suspensions that are used in the detectors like LIGO and Virgo have increased thermal noise. As a result, KAGRA will be using sapphire mirrors and suspension elements. Sapphire has a low mechanical loss at room temperature and the it's mechanical loss at cryogenic temperatures decreases by approximately one or two orders of magnitude from that at room temperature. The fact that this system incurs a smaller mechanical loss and that it operates at cryogenic temperatures means that using sapphire at cryogenic temperatures will achieve a thermal noise amplitude one to two magnitudes lower than that incurred by sapphire at room temperature [6].

The Einstein Telescope is a European interferometric gravitational wave detector. It is currently in its design phase. The main feature of ET is the creation of an observatory holding more than one detector, allowing it to detect both high and low frequency ranges. ET will also operate underground to reduce seismic noise interference. Only the low frequency detector will operate at cryogenic temperatures (approximately 10 K). It will have the same Michelson Interferometer configuration but will have 10 km long Fabry-Perot arm cavities and use either silicon or sapphire test masses and suspensions [6].

These changes to the current systems, like cryogoenically cooling it and moving it underground, that LIGO, Virgo, and GEO use will help to reduce sources of noise and improve detection accuracy. Not only will operating underground reduce mechanical disturbances such as seismic or acoustic noise but also the environmental impact would be less, both visually and in terms of restricted access for people and wildlife. [1] Separating the masses longer distances apart will also improve sensitivity. This is due to the fact that "for optical path lengths small compared with the wavelength of the gravitational wave...the phase shift is proportional to the length of each arm." [1] It can then be determined that by increasing the arm length and by bouncing the light back and forth many times in each arm before recombination at the beamsplitter, we can improve the sensitivity of our detectors. ET will implement this by making the arms 10 km long as compared to the current 4 km long arms in the LIGO detector.

Cooling the system to cryogenic temperatures will also help to improve the sensitivity because it will provide lower thermal noise in the suspensions.

"The strongest gravitational waves, those from astrophysical sources such as neutron star binary coalescence, supernovae, or black hole formation, are expected to produce strains of 10^{-21} or smaller. This means that gravitational wave detectors must meet daunting performance specifications if success is to be achieved. Simply to register such small spatial perturbations requires measurements of unprecedented precision. Simultaneously, the test masses, which must be free to respond to the gravitational wave, must also be isolated to an unprecedented degree from other disturbing influences." [7]

However, to achieve these cryogenic temperatures, a cryostat is needed. Currently at the University of Glasgow, the Institute for Gravitational Research group is working on a silicon suspension prototype that uses a pulse-cooled cryostat and will test silicon test masses.

D. Glasgow cryogen-free cryocooler

As mentioned before, there are several noise sources that limit the sensitivity of gravitational wave detectors. One major one is thermal noise. Thermal noise can be investigated by measuring the mechanical loss of the system. Mechanical loss is the sum of all losses from different types of dissipation, such as thermoelastic loss and surface loss. Operating at cryogenic temperatures will reduce magnitude of thermal noise and using silicon will result in less dissipation.

Currently at University of Glasgow, IGR staff and students are developing a small scale prototype with a silicon test mass of one kilogram. This mass will originally be suspended from ribbon fibres but will ultimately utilize the circular cross section fibres grown via the Laser Heated Pedestal Growth technique. The prototype will operate with one 1 kg suspensions and will be cooled using a pulse-cooled cryocooler. The IGR group wants to measure the mechanical loss and wants to keep the suspension reasonably isolated from seismic noise in order to make mechanical loss measurements not limited by this due to coupling.

Figure 3: The Leiden Electronics Cryostat at the University of Glasgow

In the figure above the small frame has a laser and photodiode. The laser shines in through a small viewport, is reflected off a silicon piece, and the amplitude of motion of the reflected spot is recorded using the photodiode.

II. VIBRATION SPECTRUM CONCEPT

"The extent to which long baseline interferometric detectors can be operated with reasonable sensitivity at the lower end of the frequency spectrum will depend crucially on the level of seismic and mechanical isolation achievable." [1] The design of a vibration isolation system must allow for vibrations which may be ground borne, air borne, or structure borne, and which may arise either outside the detector (i.e. environmental noise including seismic noise) or associated with the detector (vacuum pumps etc.).

I will be using two different 3-axis accelerometers in my experiment in order to discern information about these vibrations and find out at what frequencies different parts of the cryostat are oscillating.

III. EXPERIMENT

For the vibration spectrum test I used two accelerometers, ADXL345 (digital accelerometer) and ADXL354 (analog accelerometer). [10][13] I connected them both to an Arduino/Genuino Uno board which functioned as a serial port and ran the data to a program in MATLAB. I have hooked them up according to the following diagrams in Figures 4 and 5. The code for the serial connections from the Arduino to MATLAB can be further explored in the Appendix B.

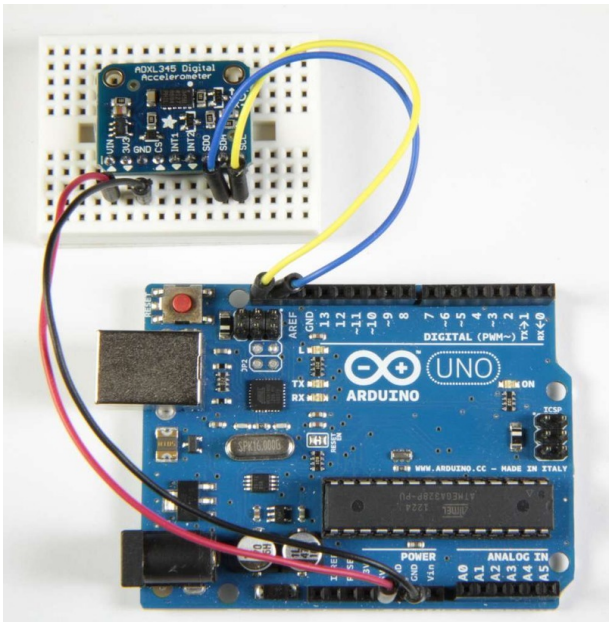

Figure 4: A diagram depicting the wiring of the ADXL345 accelerometer to the Arduino Uno board. This figure was taken from Bill Earl's article on adafruit.com. [9]

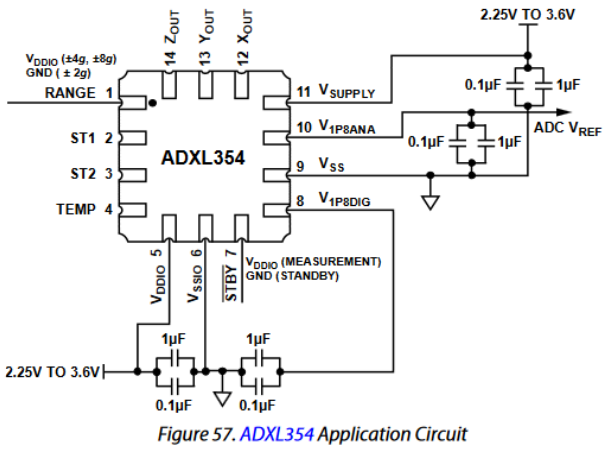

Figure 5: A diagram depicting the wiring of the ADXL354 accelerometer to the Arduino Uno board. This figure was taken from ADXL354 data sheet. [10]

But before we could take any data, we needed to calibrate the accelerometers.

A. Methodology

The goal of this experiment was to find information on the acceleration of the cryostat. This will provide information to the IGR group about what kind of sensitivity we have and how to build the suspensions to meet that sensitivity. This in turn will help the group find the optimum suspension geometry for the test mass in the future.

1. *Vibration analysis*

Vibration analysis of the cryocooler will tell us what noise sources are present within our system, whether that be from the cryocooler, compressor, turbo and ragh pumps, etc. It also allows us to explore noise in silicon as an optic which until now hasn't been done before. I will be using two accelerometers and first calibrating each one.

Checks and calibration tests

The purpose of the calibration tests was to find the sensitivity of each accelerometer. The calibration test consisted of hooking up a speaker system to the accelerometer and making it oscillate at a known frequency and amplitude.

First we ran the accelerometer with a few different sine wave frequencies so we could estimate the sample rate and the reproduciblity. Following one test through the process, I first drove the accelerometer with a sine wave of amplitude 5 Vpp and oscillating at 4 Hz. The Arduino program is set to output three columns of data (x, y, and z accelerations) every 0.1 millisecond. This data is then sent to MATLAB where it is converted to numbers and separated into three columns of data written into a spreadsheet. (See appendix for further detail.) An example of the outputted data is shown in Figure 6.

x	y	z
-2.23591637	0.86298522	-9.29670524
-2.23591637	0.86298522	-9.29670524
-2.23591637	1.09834480	-9.80665016
-2.27514290	0.54917240	-9.68897056
-2.27514290	0.47071924	-9.53206443
-2.23591637	0.74530549	-9.72819709
-2.23591637	0.98066501	-9.72819709
-2.19668960	0.94143848	-9.72819709
-2.27514290	0.90221195	-9.72819709
-2.19668960	0.78453207	-9.80665016
-2.27514290	0.47071924	-9.61051750
-2.27514290	0.54917240	-9.76742362
-2.23591637	0.78453207	-9.72819709
-2.27514290	1.01989161	-9.72819709
-2.19668960	0.94143848	-9.68897056
-2.27514290	1.09834480	-9.68897056
-2.23591637	0.86298522	-9.76742362
-2.27514290	0.50994582	-9.68897056
-2.23591637	0.50994582	-9.68897056

Figure 6: This is a snapshot of some of the data collected for a run at 4 Hz. To give a sense of scale, there were around 5,100 data points collected for around a minute of testing.

I then define the time domain using the sampling time. The sampling time was found within the code by measuring how long it took to collect a certain number of data points. Averagely, it took 0.03783 seconds per data point. This helped to create a calibrated time axis on which I then plotted the accelerations in the x, y, and z directions. Since the z-direction is facing up on the accelerometer, it has an average acceleration of around 9.8 m/s^2 when stable due to gravity as compared to the other axes which have an average of around 0 when stable. To account for this, we subtract the mean from the data for each axis and then to visually compare them, I separated them by adding a value of 1 to all the x-axis accelerations and subtracting a value of 1 from all the z-axis accelerations. (See Figure 7)

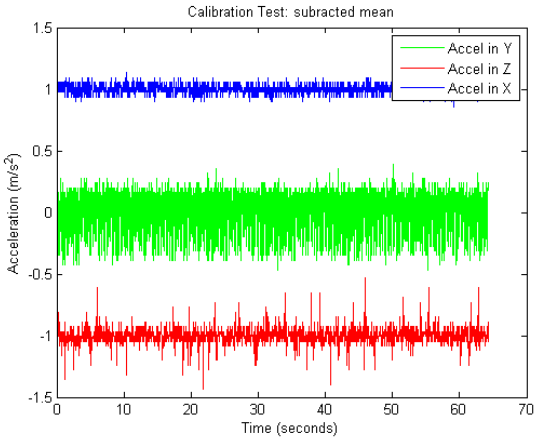

Figure 7: Subtracted means of data at 4 Hz

To then adjust for any sloping, I took the polyfit of the subtracted mean data (the one without the ± 1 adjustment for visualization) and plotted that. An example of the polyfitted data is in Figure 8. I did not offset the polyfitted data. (See Figure 8)

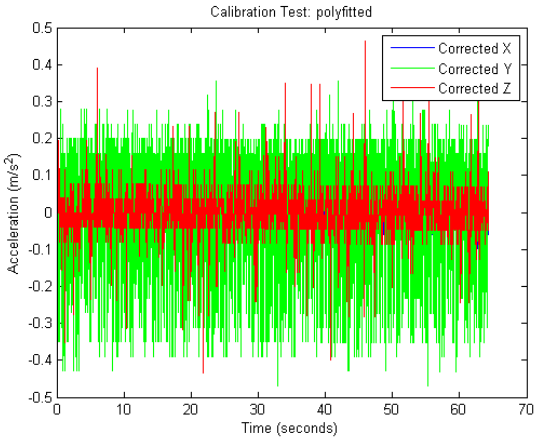

Figure 8: Polyfitted data at 4 Hz

Finally I take a Fourier transform of the data in order to convert the data to a frequency spectrum. We then had a spread of the amplitudes of each frequency in $(\mathrm{m/s^2})/\sqrt{(\mathrm{Hz})}$. (See Figure 9)

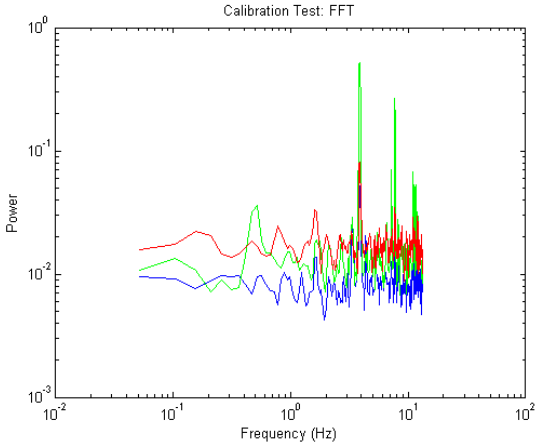

Figure 9: Fast Fourier Transform of data at 4 Hz

Figure 9 shows there is a peak at 4 Hz which is the frequency we were driving the accelerometer with so this is what we expect. There is also a peak at 8 Hz. This is an example of coupling where you will see the driving frequency (4 Hz), double that (8 Hz) and theoretically double that (16 Hz) but this accelerometer isn't sensitive enough to detect that higher frequency accurately. This process was repeated in increments of 2 Hz up to 12 Hz. At 12 Hz this accelerometer stops being as reliable. This is due to the sampling time. If the accelerometer was able to detect faster, then it could detect frequencies higher than 12 Hz. Past that point, the frequency spikes that it shows are due to coupling.

Another calibration test that was performed was holding the accelerometer in hand and rotating it 90° every 1 second, alternating whether the y or z axis was facing up. This was to test whether it could detect low frequencies like the 1 Hz square wave we were making. The polyfitted data in acceleration vs. time is shown in Figure 10.

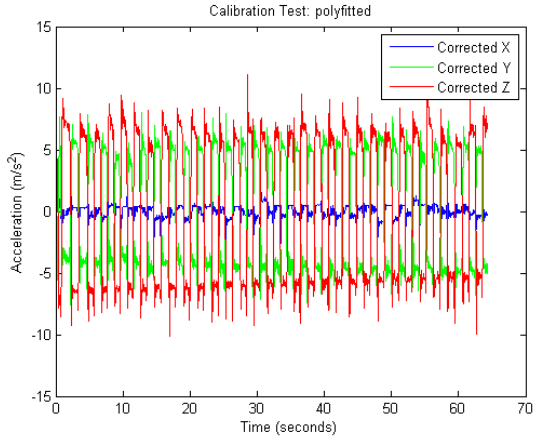

Figure 10: Polyfitted data of 1 Hz square wave

The FFT of this data worked well, producing a strong

peak around the expected 1 Hz. Of course it is not exactly at 1 Hz because the signal was produced by hand and there is some error within that. However, it was close enough to show that it can detect low frequencies as well. The peak seen in Figure 11 occurs at 0.5 Hz. This could also be due to reverse coupling in which case instead of seeing doubles of the driving frequencies, one can expect to see halves. This is not common usually but in imperfect systems it becomes a more probable occurrence.

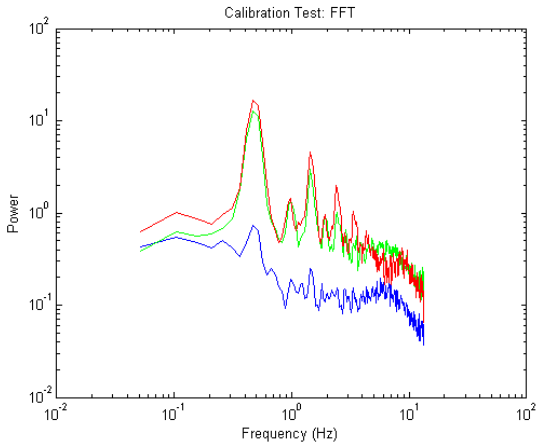

Figure 11: FFT of 1 Hz square wave

Additionally, I verified that the values that the accelerometer was giving were accurate by calculating the theoretical maximum acceleration of the simple harmonic oscillation of the voice coil. Using a camera and a ruler, I determined that the overall peak to peak displacement of the accelerometer at that amplitude was 1.5 mm. Using this information and the fact that the frequency of oscillation is known to be 4 Hz, I calculated the that maximum acceleration should be $\pm$ 0.47 m/s^2. The results were consistent with what we were getting for acceleration values for the calibration tests. In Figure 8, the maximum acceleration values are around 0.47 m/s^2 in magnitude on the negative side. However, on the positive side, the maximum values only reach around 0.2 m/s^2 in magnitude. This is due to the accelerometer's sampling rate or how fast it can communicate data over the serial port. The accelerometer is seeing the smooth sine wave more as a triangle wave thus bringing the maximum acceleration down.

This tells us that there is some error that comes with the accelerometer data, however the values can be trusted generally and still give us a good idea of how the system is behaving with respect to itself and the other axes.

Now that we know that the ADXL345 accelerometer has a sensitivity of 12 Hz, we are now ready to use it to conduct vibration spectrum test of the cryostat itself.

Vibration tests

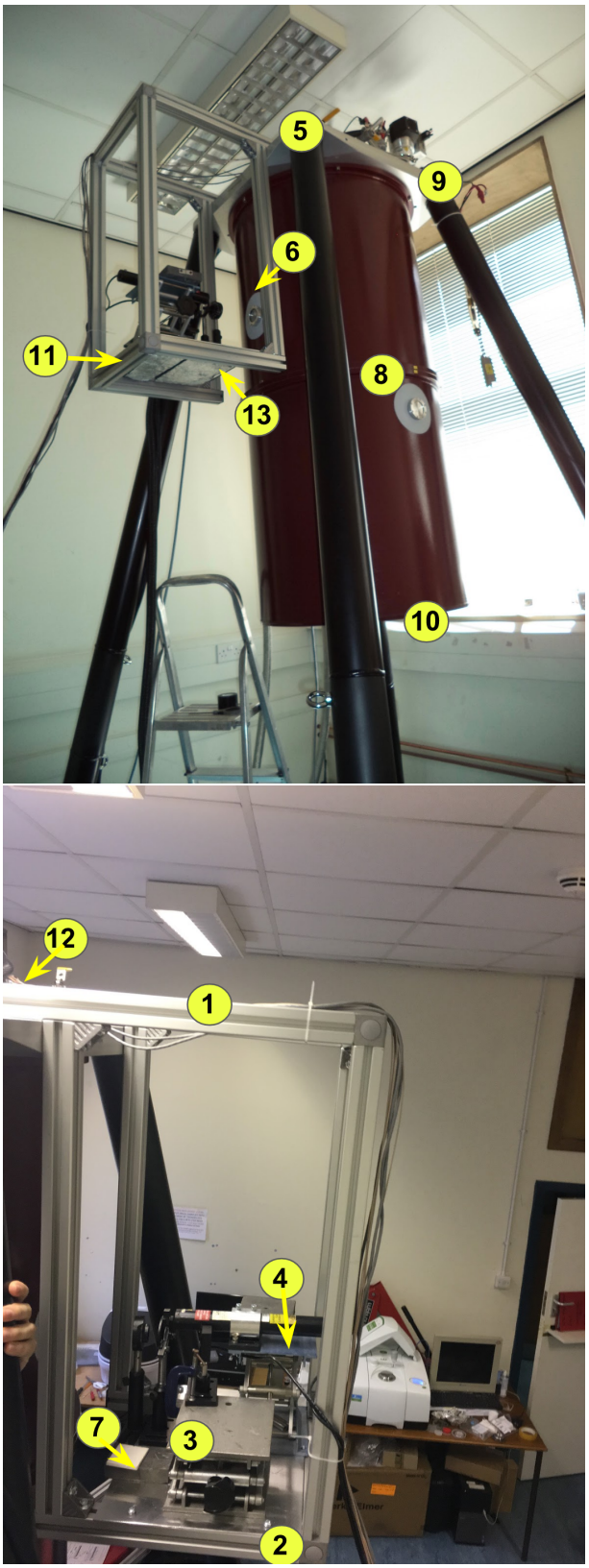

Figure 12: Diagrams of testing positions on the outside of the cryostat

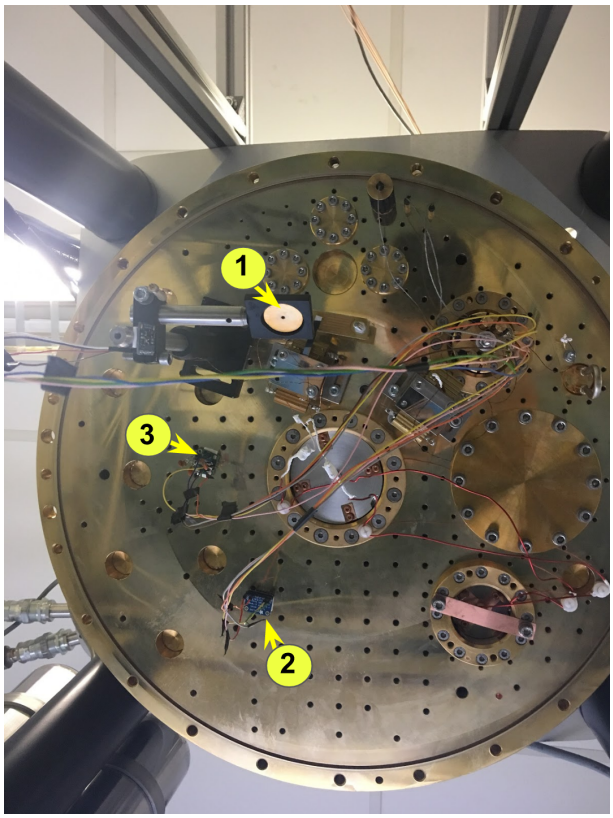

Figure 13: Diagram of testing positions on the inside of the cryostat. Position 1 (ADXL345) is on mirror lever that hangs down from the base plate. Positions 2 and 3 are directly on the base plate and contain an ADXL345 (2) and an ADXL354 (3)

I used each accelerometer to take vibration data at various points on the outside frame and the inside body of the cryocooler. Figures 12 and 13 show diagrams of the locations on which I collected data.

I went through the same process as the calibration tests to produce a subtracted mean and polyfitted data vs. time graph and a FFT amplitude vs. frequency graph. A few examples of data taken with the ADXL345 accelerometer are below.

The tests are then repeated with the ADXL354 accelerometer and the results are compared.

2. *Cooling time analysis*

Cooling time analysis of the cryocooler consisted of measuring the vibration spectrum of the inside of the chamber periodically as the cryostat cooled. The accelerometers were attached to the cold plate inside the system as seen in Figure 13 and originally set out to collect about a minute of data every hour.

There were some setbacks with this test due to problems with the mechanics of the cryocooler. The cooling system would automatically shut itself down after about 20 minutes due to an error of high oil temperature. The oil temperature is regulated by the water temperature and flow, however no member of IGR could find any issue with the water. Eventually some IGR staff shortened some of the tubing for the water and then the cryostat worked again. Even though there were issues with the running of the cryostat, I did manage to collect some data at various conditions. The cryostat is composed of an outer chamber (red) and two inner chambers that are a 50 K shield and a 3 K shield. Inside at the top there is a 3 K base plate on which the accelerometers were attached. Since the chamber is vacuum sealed, we had to wire the accelerometers through a pre-existing connection between the inside and the outside of the chamber. This can be seen in Figure 14. The accelerometers were attached using red tape as seen in Figure 15.

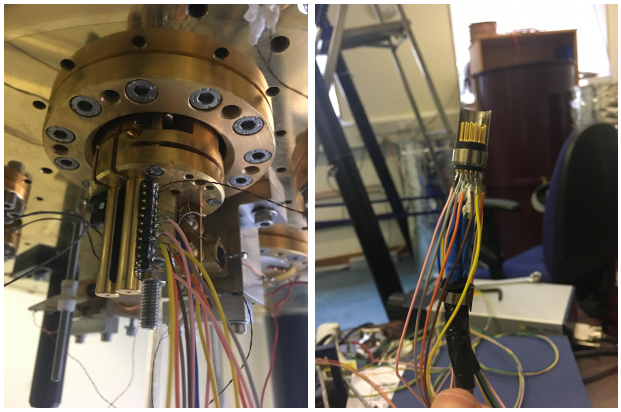

Figure 14: The inner and outer connections (respectively) for the wiring of the accelerometers inside the cryostat

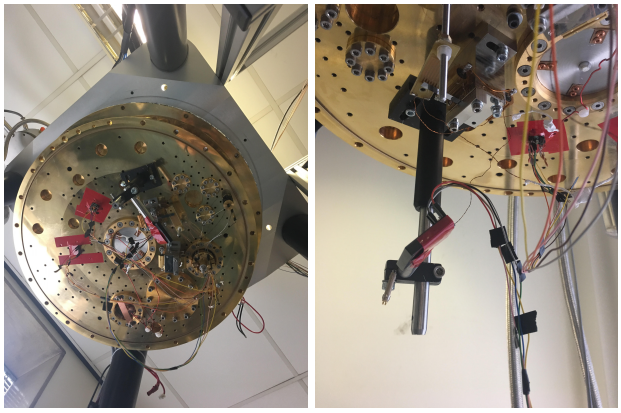

Figure 15: The inner and outer connections (respectively) for the wiring of the accelerometers inside the cryostat

I took data from each accelerometer when the cryocooler was off and the tank was open like in Figures 14 and 15. I also did the same test for when the cham-

bers were secured back on and the vacuum had just been turned on and after the chamber had been completely depressurized. I then took incremental data after the cryocooler had been turned on. We expected that eventually the accelerometers would stop working after they reach a certain temperature but the goal was to collect as much data as possible at various temperatures as it cools until the accelerometers break.

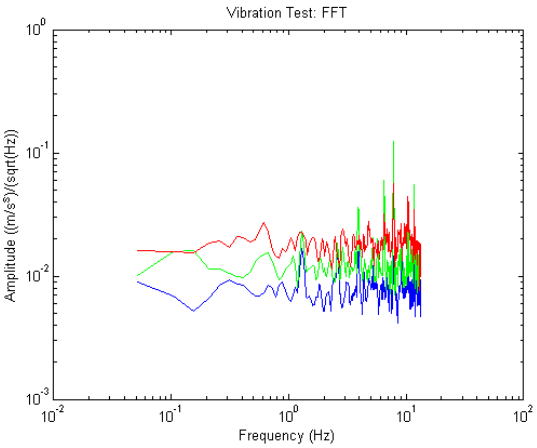

Figure 17: Position 1

B. Results and analysis

From the data taken, a few observations can be made. Following will be a collection of notable graphs collected from the experiment and what can be found from them. Please refer to the diagram in Figures 12 or 13 above or a bigger version in the Appendix A for a visualization of the position references.

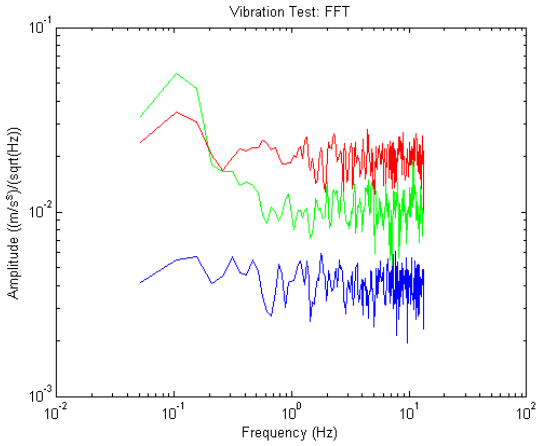

Figure 16: Position 1, cryocooler off

Figure 16 shows frequency spectrum of vibration obtained at position 1 when the cryocooler is off. This will serve as our reference plot for any noise induced in the system from the cooling mechanisms. The noise present here would be from the vacuum pumps, which are constantly running, background noise from the room, or resonance vibrations within the materials themselves.

Figure 17 is from the same position as Figure 16 but now the cryocooler has been turned on. Notice defined frequencies at 4, 7, and 8 Hz, predominantly in the Y (green) and sometimes in the Z (red) directions. This tells us that because of how the accelerometer is attached to the system that at this point the frame is mostly shaking horizontally back and forth with a bit of bouncing up and down at specific frequencies.

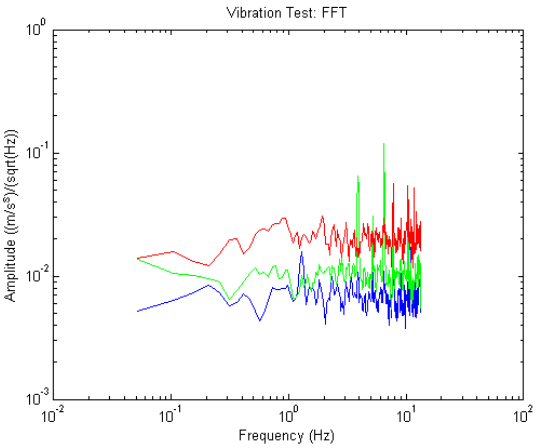

Figure 18: Position 2

Figure 18 was taken from position 2 and from this one can really see the the Y-direction (green) is really shaking noticeably at 4 and 7 Hz and there is also some notable shaking in the Z-direction around 8 and 10 Hz.

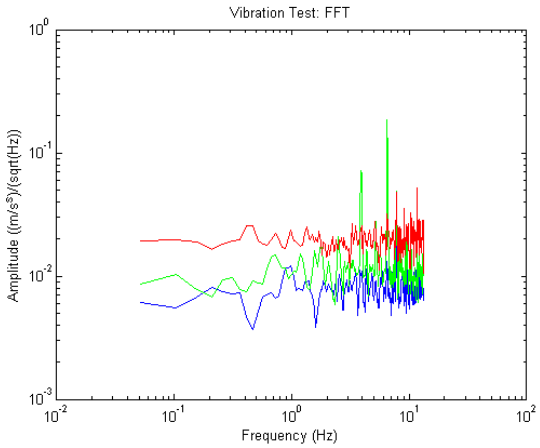

Figure 19: Position 3

Position 3 confirms that the system is vibrating consistently at 4 and 7 Hz in the Y-direction which in this case is a back and forth motion of the frame.

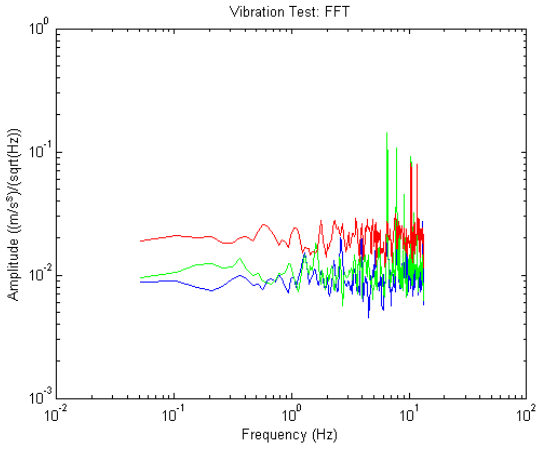

Figure 20: Position 4

As seen in Figure 20, there is definitely vibration at 10 Hz in both the Y and Z directions at position 4. There is also dominating frequencies in the Y direction at 7 and 8 as well. Also as seen by the amplitudes, the spike in X is almost as significant as the Y so that says in this location, the system is bouncing up and down almost as much as it is shaking back and forth.

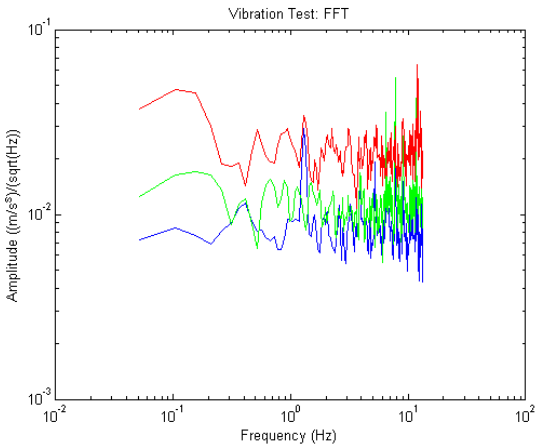

Figure 21: Position 5

Position 5 shows us a vibration spectrum with no real dominating frequencies below 12 Hz. This is indicative of a relatively quite location on the cryostat that is not shaking much.

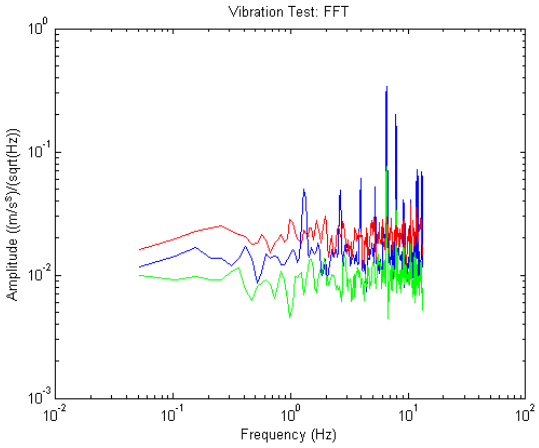

Figure 22: Position 7

Position 7 is shaking predominantly in the X direction. This makes sense as the X-direction would be the defined Y-direction in most other positions. This is just due to how I fastened the accelerometer to the equipment. In this position, the dominating frequencies are 7 and around 10 Hz.

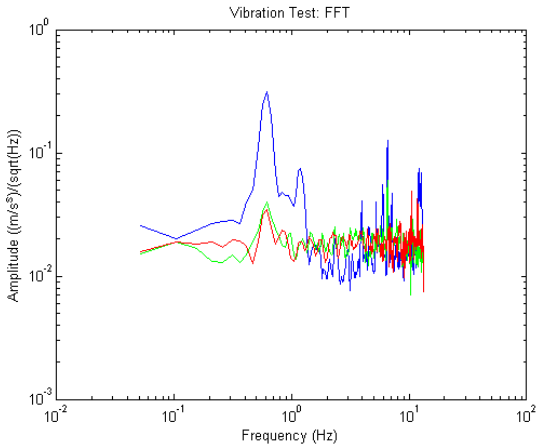

Figure 23: Position 11

Figure 23 was collected from position 11 and had high amplitudes at 3 and 7 Hz with a spike at the end near 10 Hz.

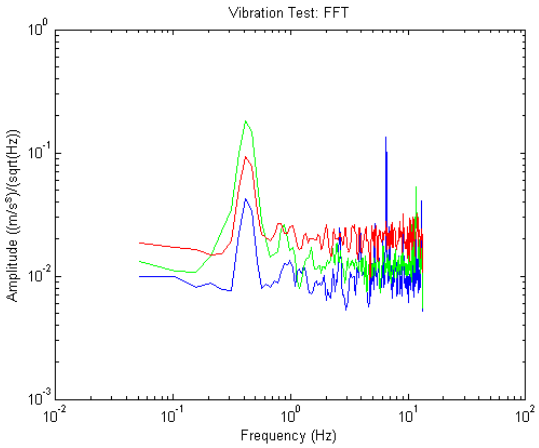

Figure 25: Position 13

Position 13 yet again shows a spike at 7 Hz which has been a reoccurring frequency around the system.

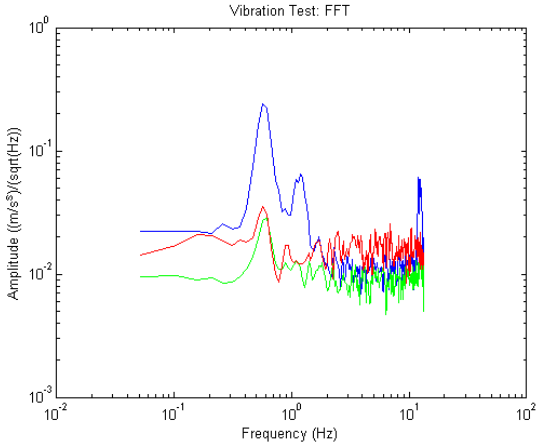

Figure 24: Position 11

Figure 24 is the data from position 11 as well (see Figure 23), however this time with the system turned off. As one can see, the spike around 10 Hz is still present which informs us that this vibration is not caused by the cryocooler being on but rather another source, perhaps a resting resonance frequency of the system at this point.

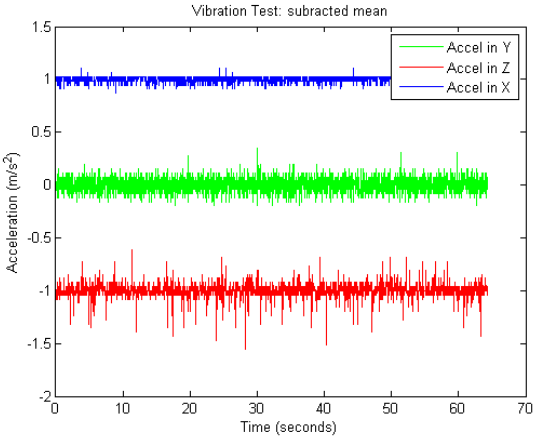

Figure 26: Position 3

Typically the subtracted mean graph for the data collected from the frequency scans looks like this. Figure 26's specific data came from position 3 on a pedestal on base plate of the frame. This is how most of the mean graphs turned out. Below I will also include some notable others.

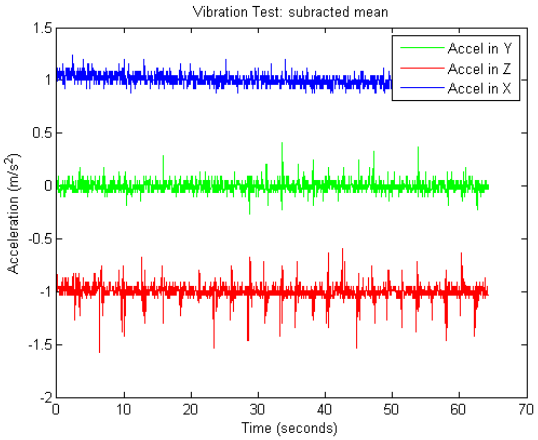

Figure 27: Position 6

Position 6 yielded vibrations that were very present in the Z (red) direction, meaning the system was bouncing up and down a lot on the laser window on the shell of the cryostat.

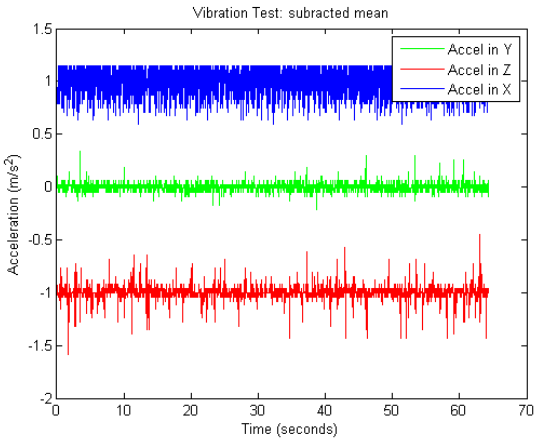

Figure 28: Position 7

As noted in Figure 22, the base plate for the external laser is very noisy in the X-direction, meaning it is shaking back and forth the most on the frame. This can be seen and verified here by clear contrast to vibrations in the other directions.

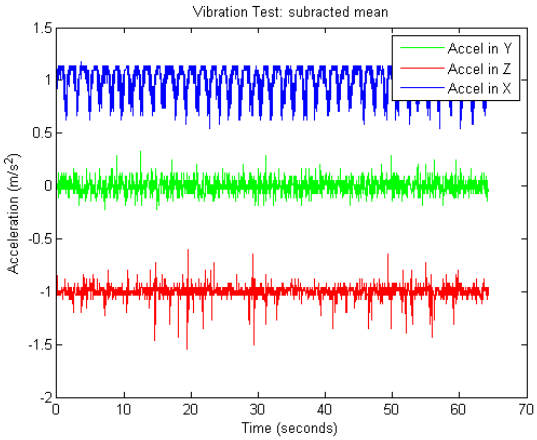

Figure 29: Position 11

As mentioned above, this observation can also be seen by the mean graphs. Here, in Figure 29, one can see the clear dominant vibrations in the blue X-direction.

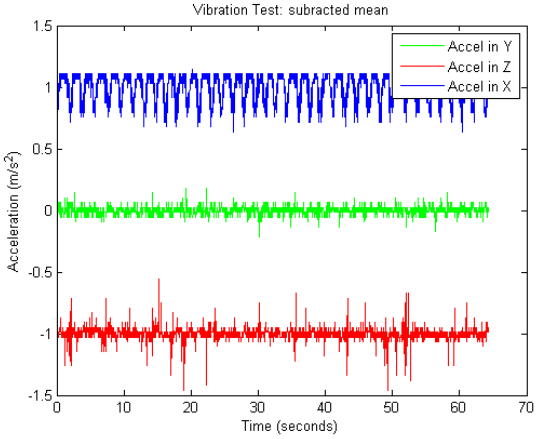

Figure 30: Position 11, cryocooler off

But as you can see, when the cryocooler is turned off, the same vibrations in the X-direction are still present.

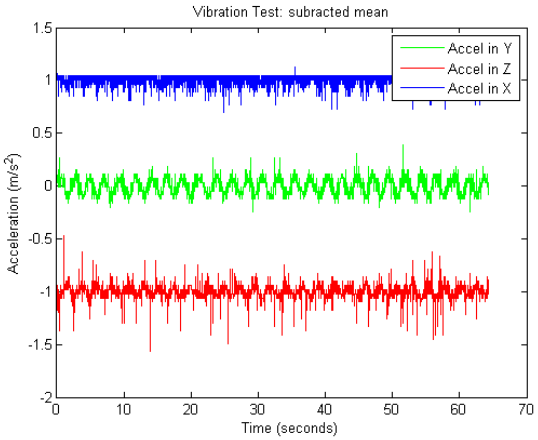

Figure 31: Position 13

Position 13, the base plate, is an important graph to show as well because there is almost a visible sine wave present in the vibrations of the Y and Z directions. This indicates that the cryostat is oscillating slowly but consistently.

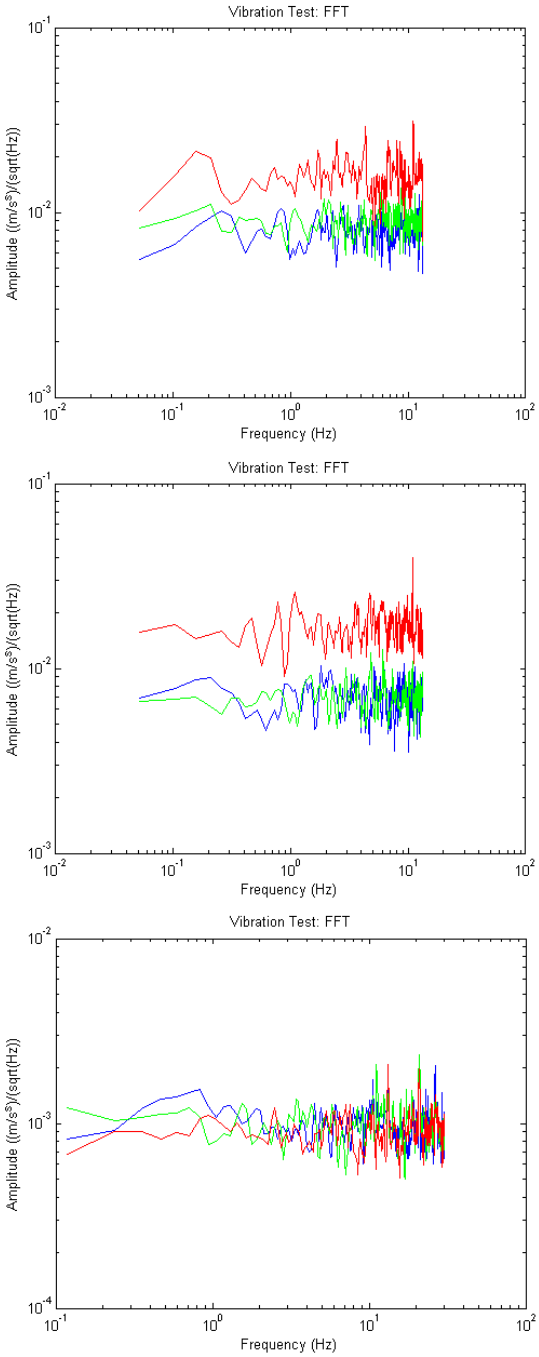

Figure 32: Frequency spectrum of accelerometers 1, 2, and 3 with cryocooler, vacuum pump, and outer shields off

For the measurements the were taken inside the cryostat, here's what was discovered. The results for the initial test of the cryocooler off and open can be found in Figure and in comparison, the results of the cryocooler off but closed are in Figure 32.

To see if there was any difference, I think collected data from after the three shields were secured on again and before we turned the vacuum pump on. (See Figure 33)

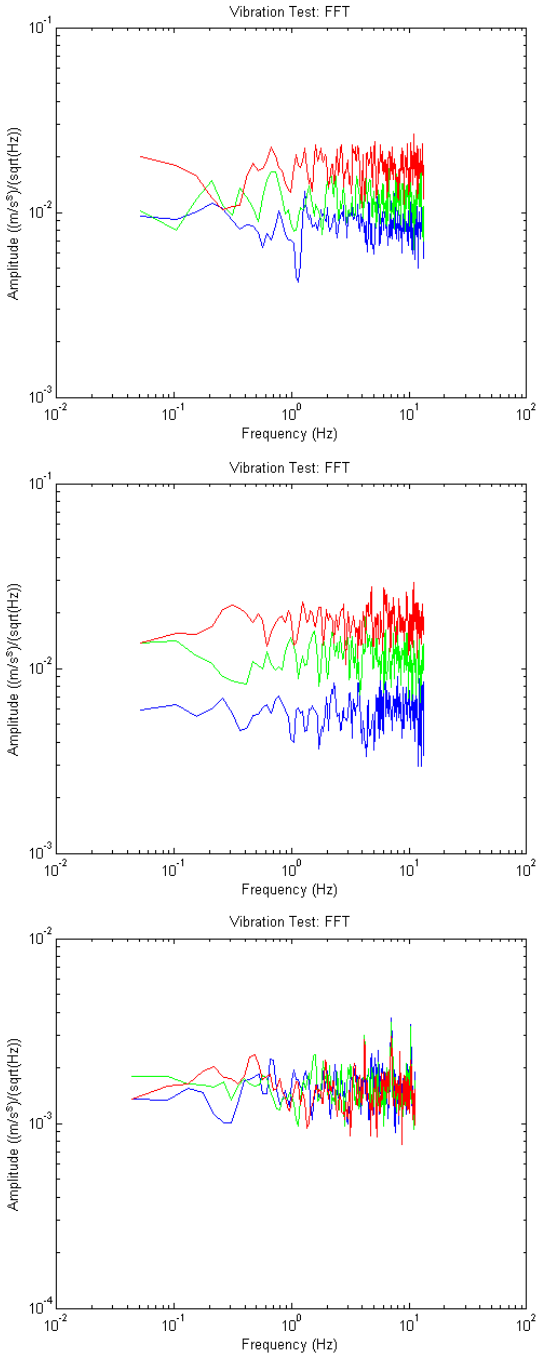

Figure 33: Frequency spectrum of accelerometers 1, 2, and 3 with cryocooler and vacuum pump off and outer shields on

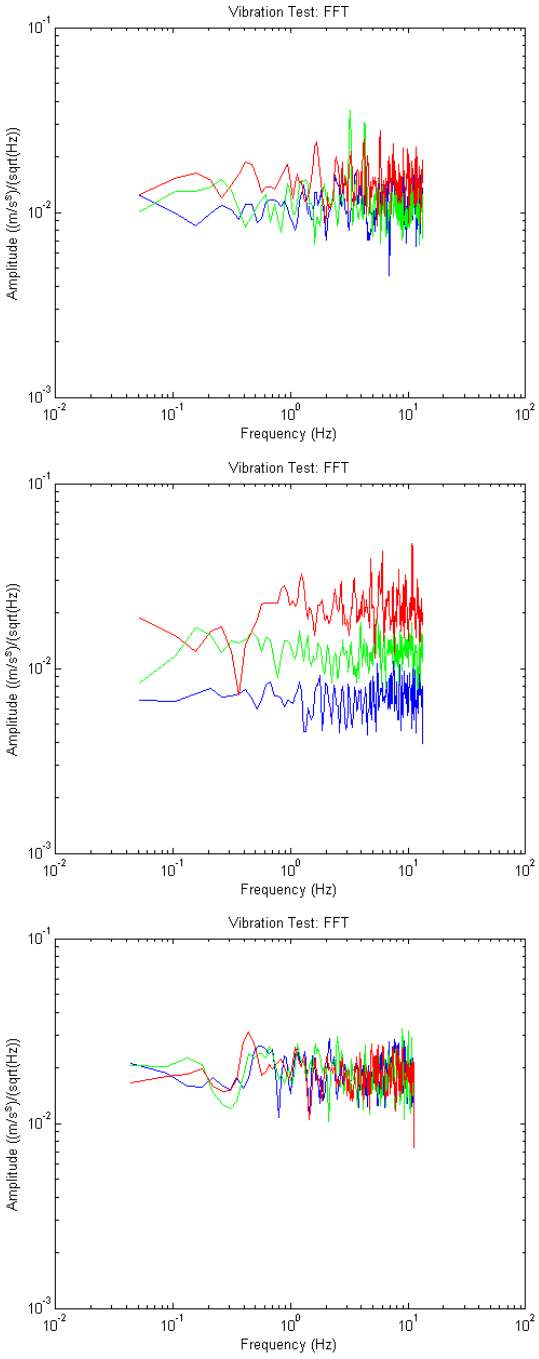

Figure 34: Frequency spectrum of accelerometers 1, 2, and 3 with vacuum pump and outer shields on with cryocooler off

From this data it was concluded that the shields being on there did not add any significant frequencies to the system. After, we turned the vacuum pump on until the pressure on the inside of the tanks reached a magnitude of $10^{-}02$ mbar. This process took about 24 hours. The data from after the vacuum pump had been on for almost 24 hours can be found in figure 34.

There is a contribution from the vacuum pump seen by the digital accelerometers at 3, 4, and 6 Hz seen in Position 1 (the suspended mirror) and around 10 Hz which is felt by accelerometers 2 and 3 on the base plate.

When the cryocooler was turned on, the initial temperature was at 297.1 K. It took many trials get all three accelerometers data around the same temperature and time because of the complications with the heating of the

oil in the cryostat. After shortening the tubing for the water cooling system that regulates the oil temperature, the cryostat was back in operation and ran consistently. Additionally, during this trial period, I had begun to edit the Arduino code to see if I could get the accelerometers to have a higher sampling rate by increasing the rate at which the data is communicated across the serial port. At this time, I had increased the sampling time to 0.010265 seconds/data point for the analog accelerometer and one can see the sensitivity has increase and it can now detect signals up to about 17 Hz. This data can be seen in Figure 35.

At T=0 (temp: 297.30 K), on accelerometer 1, on the mirror suspension, there are peaks at 3, 5, 7, and 10 Hz that are very defined. Since the peaks at 3 and 5 Hz were present before the cryocooler was turned on and after the vacuum was turned on, we can attribute peaks 3 and 5 Hz to be coming from the vacuum and peaks at 7 and 10 to be coming from the cryocooler. This is consistent with the results from the outside of the cryostat in that there vibrations at 7 Hz was also felt. The digital accelerometer on the base plate feels minor vibrations at 3, 6, and 12 Hz so we are definitely experiencing some coupling here. The analog accelerometer doesn't appear to see the same frequencies and has its most significant vibration occurring around 2.5 Hz.

At T=1 (temp: 279.97 K) the results can be found in Figure 36. The peaks on accelerometer 1 have become very distinct and strong at 1, 1.5, 3, 5, 6, 7 and 12. Accelerometer 2 seems to have a slight peak at 4 Hz but this is not confirmed by accelerometer 3 which may have a slight peak at 2 Hz.

I took data again at temp: 151.51 K (T=2) and temp: 130.88 K (T=3) which can be seen in Figures 37 and 38.

In another effort to increase the sensitivity of the analyzers, I have reduced the number of significant figures of the data from 8 to 4 in the code and for the analog detector, I have tried reading each axis individually. Both of these options has sped up the sampling rate and increased the sensitivity. An example of the data taken from each axis individually can be found in Figure 39.

Another test to increase the sensitivity was to increase the baud rate of the serial port. I had much success with this attempt; the results of this effort can be seen in Figure 40 where I have adjusted the baud rate to 2000000 instead of the previous 9600 setting. I then had to adjust all the time constants for each accelerometer and also took 1 minute of data for each run. In addition I have also ran each axis on accelerometer 3 individually as seen in Figure 41.

The reason for the curving in the digital accelerometers that can be seen in Figure 40 comes from anti-aliasing low pass filters that are built into the accelerometer. The sensitivities are very high for both types of accelerometers now. The digital ADXL 345 accelerometers can detect up to 100 Hz and the analog ADXL 354 accelerometers can detect up to almost 200 Hz and when we read each axis individually, we can detect up to 300 Hz.

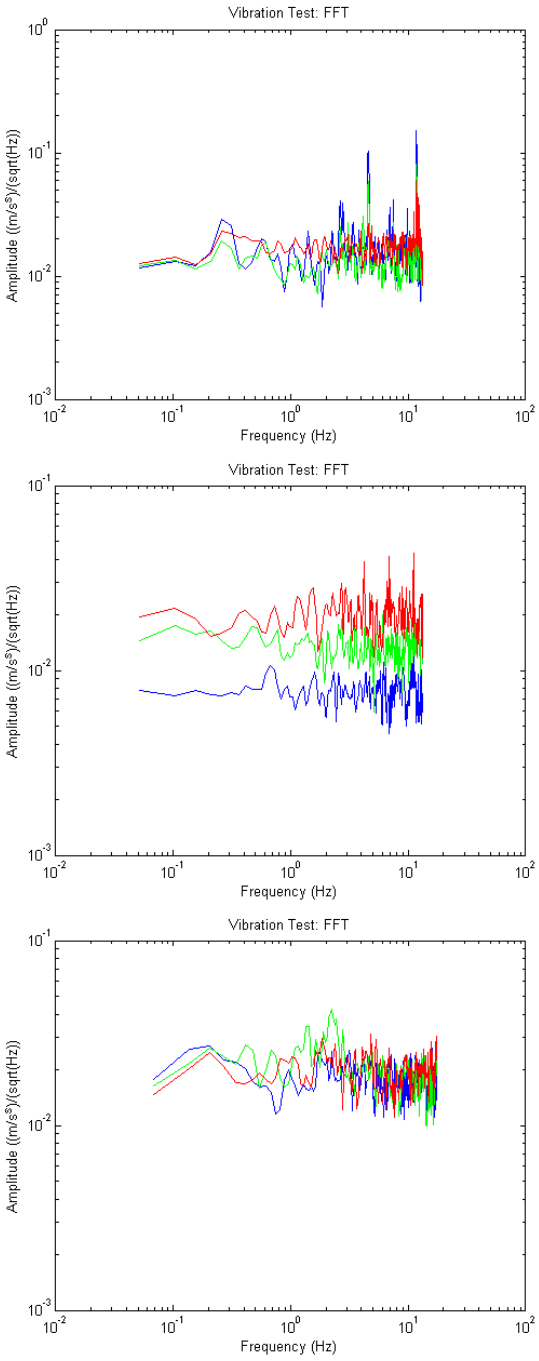

Figure 35: T=0 (temp: 297.30 K) Frequency spectrum of accelerometers 1, 2, and 3 with cryocooler, outer shields, and vacuum pump on

From this data, we can see that in accelerometer 1, on the mirror, there are vibrations at 5 and 9 and some higher ones at 35, 50 and 60 Hz. The digital accelerometer on the base plate, accelerometer 2, has a singular very strong peak at 12 Hz. This spike is not present on the analog accelerometer which we would expect it to be because they are at the same position. Instead ac-

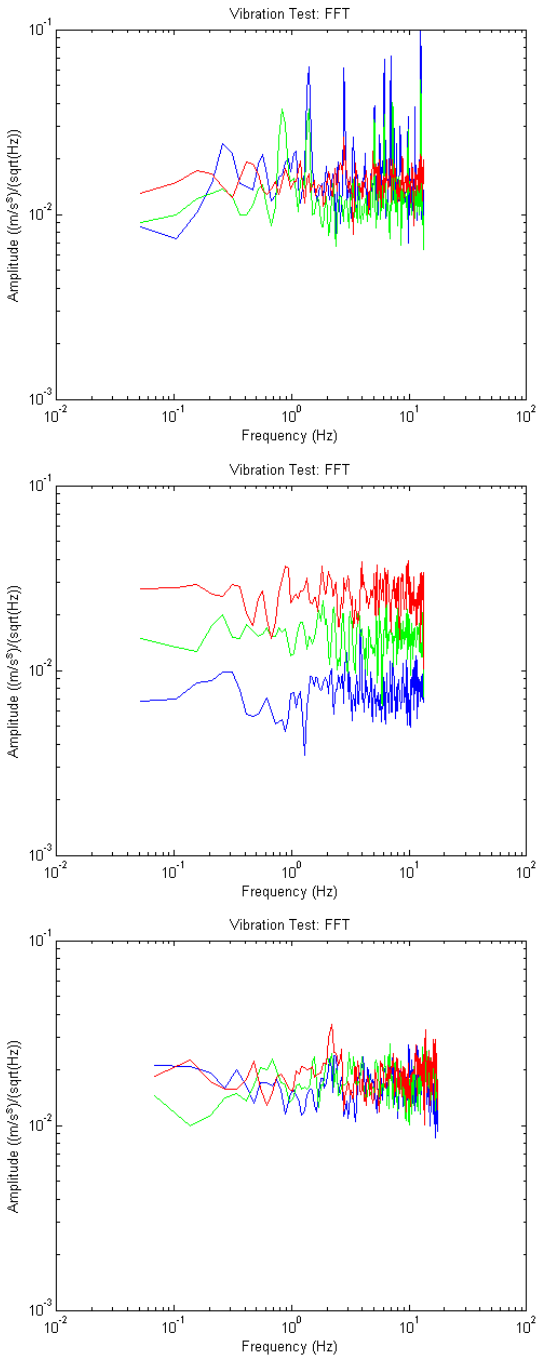

Figure 36: T=1 (temp: 279.97 K) Frequency spectrum of accelerometers 1, 2, and 3 with cryocooler, outer shields, and vacuum pump on

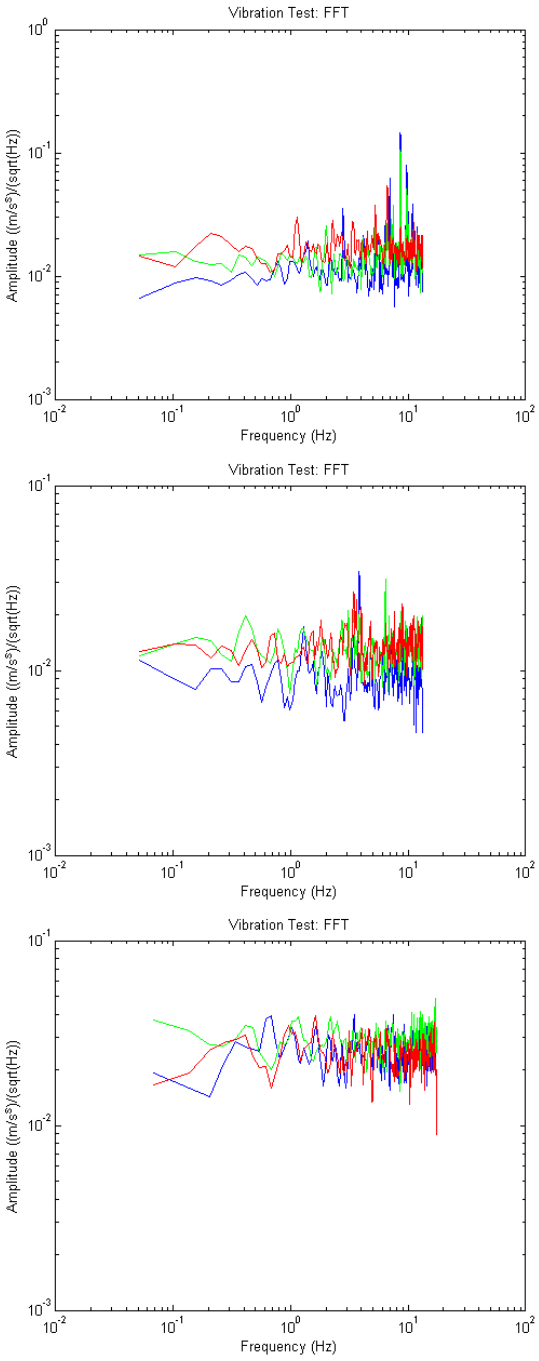

Figure 37: T=2 (temp: 151.51 K) Frequency spectrum of accelerometers 1, 2, and 3 with cryocooler, outer shields, and vacuum pump on

celerometer 3 sees peaks at 3, 5, a broad peak at 25, 60, 80, and 150. From the individual axis data we see that there is a peak at 40 in all directions and a peak at 2 and 3 Hz in the X and Y directions. There is consistently a peak between 60 and 80 Hz and at 300 Hz in all directions.

The analog accelerometer died after that at around 100 K and the digital accelerometer died around 97 K. The analog accelerometer died first because there were external capacitors exposed on it that couldn't operate at low temperatures. The digital accelerometer 1 on the mirror suspension lasted until 90 K and I was able to get two more reliable measurements out of that one before I stopped collecting data. This data can be seen in Figures

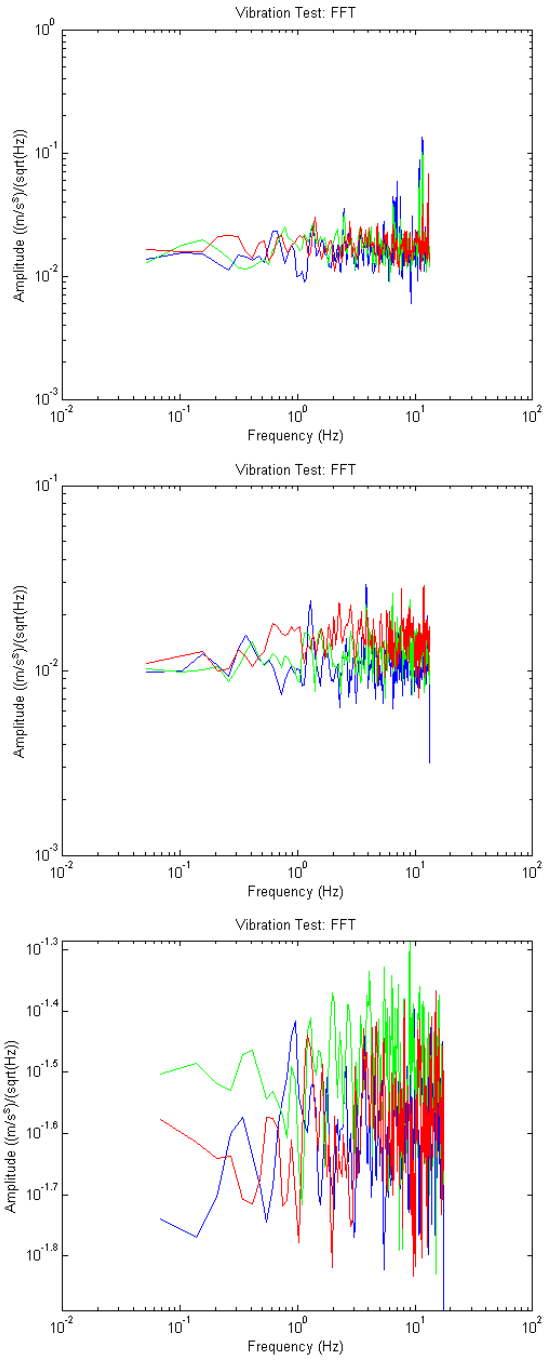

Figure 38: T=3 (temp: 130.88 K) Frequency spectrum of accelerometers 1, 2, and 3 with cryocooler, outer shields, and vacuum pump on

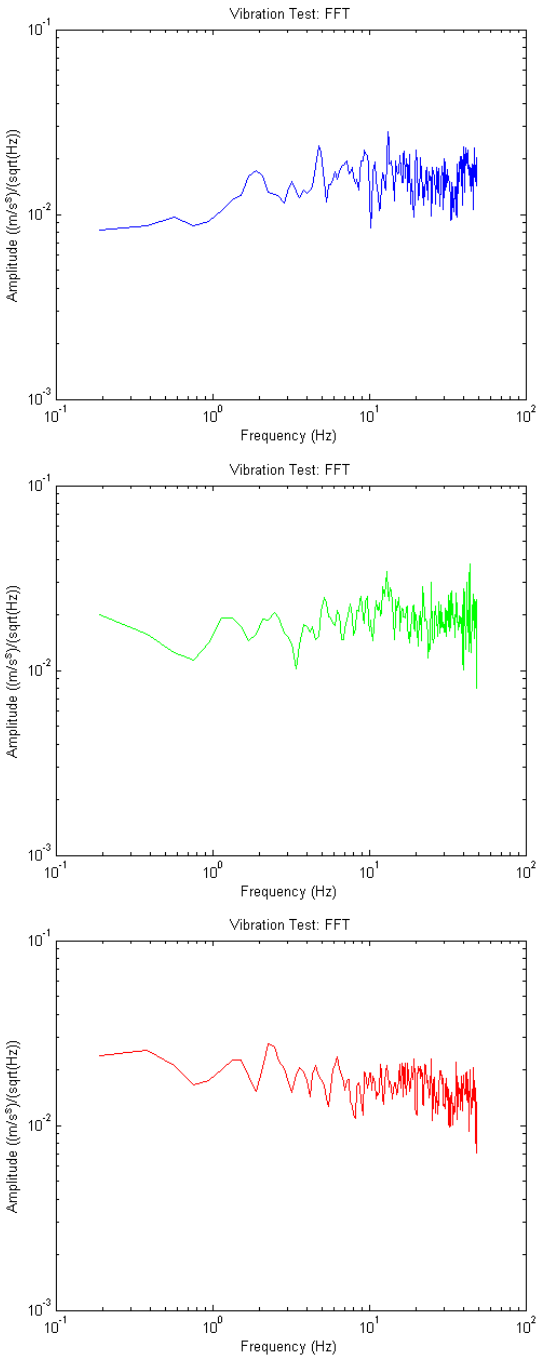

Figure 39: T=3 (temp: 130.88 K) Frequency spectrum of accelerometer 3 separated into X (blue), Y (green), and Z (red) directions with cryocooler, outer shields, and vacuum pump on

42 and 43.

These last two calculations show that the vibrations are in general decreasing as the temperature cools and that there are still peaks at 6, 12, 35, 50, and 60 Hz and eventually just 35, 50, and 60 Hz. I suspect that accelerometer 1 latest the longest because of its position. Perhaps the base plate gets significantly colder than the mirror suspension.

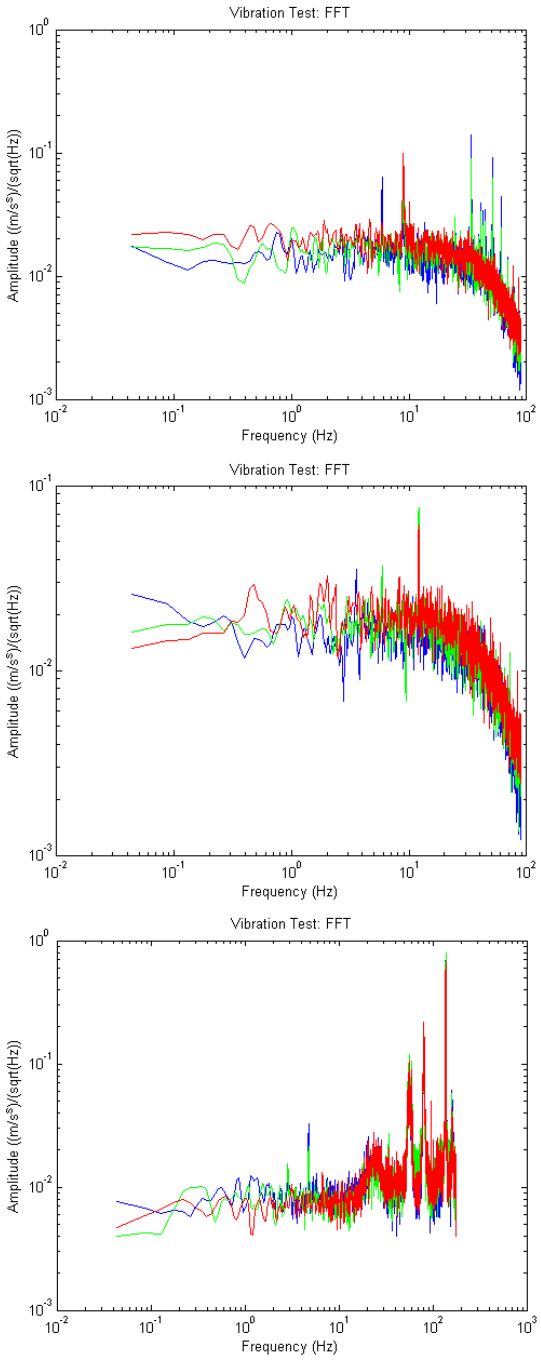

Figure 40: T=4 (temp: 115.23 K) Frequency spectrum of accelerometers 1, 2, and 3 with cryocooler, outer shields, and vacuum pump on, increased baud rate (2000000)

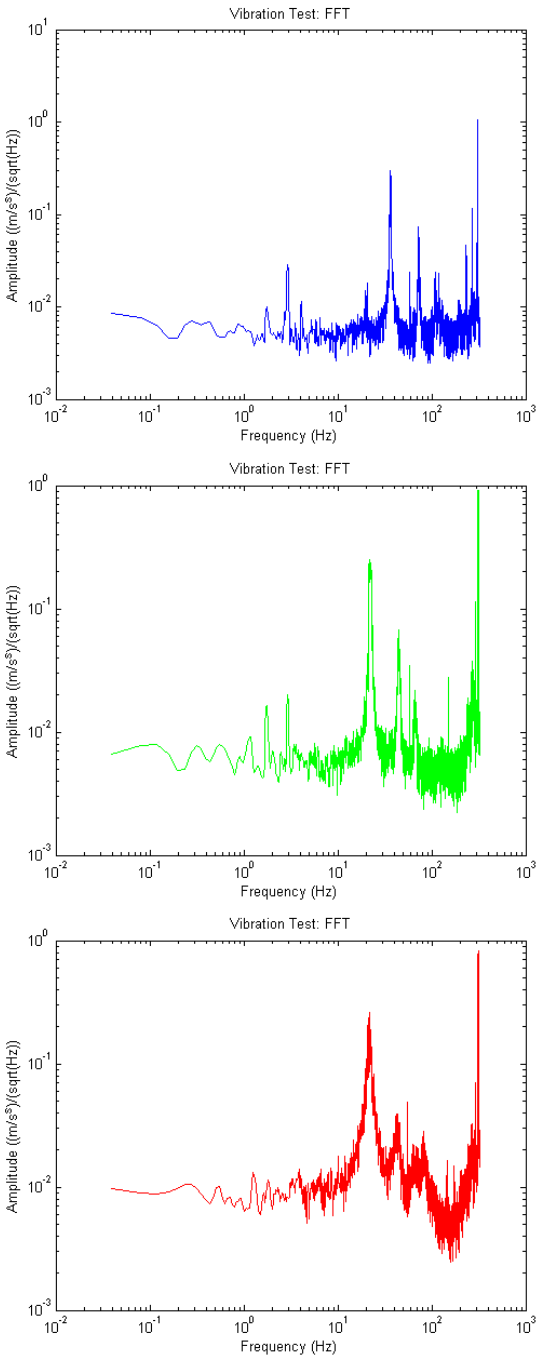

Figure 41: T=4 (temp: 115.23 K) Frequency spectrum of accelerometer 3 separated into X (blue), Y (green), and Z (red) directions with cryocooler, outer shields, and vacuum pump on, increased baud rate (2000000)

C. Conclusions

In conclusion, these various tests tell us that the system is vibrating mainly at 7 Hz all around. Additionally near the top of the frame, it is not shaking as much as the bottom which is to be expected as the frame is fixed to the stand at the top. Position 12 is the pivot point where the frame is attached and there is almost no vibration there. The furthest point away from there would be points like 11, 7, or 2 which were all very noisy. The bottom of the frame was pretty consistently shaking back and fourth at 7 and 4 Hz. The vertical vibrations also got more

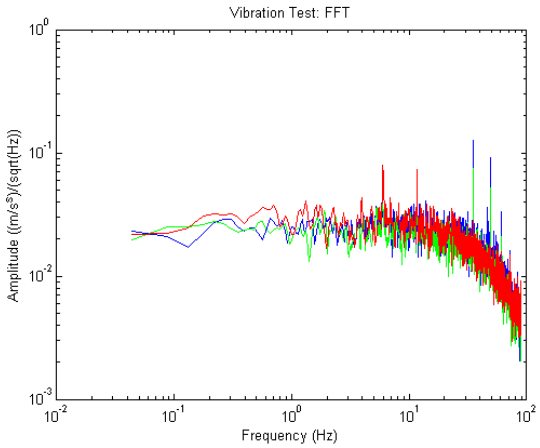

Figure 42: T=5 (temp: 96.55 K) Frequency spectrum of accelerometer 1 with cryocooler, outer shields, and vacuum pump on, increased baud rate (2000000)

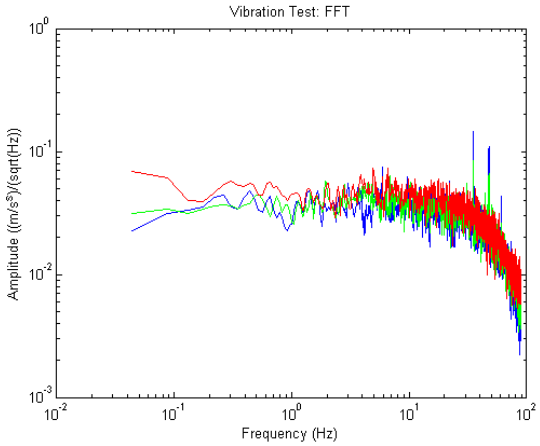

Figure 43: T=6 (temp: 90.14 K) Frequency spectrum of accelerometer 1 with cryocooler, outer shields, and vacuum pump on, increased baud rate (2000000)

present as you moved down the frame where there were noticeable vibrations around 10 and 8 Hz.

The 10 Hz signal was present even when the cryocooler was off so that noise must be coming from the resonance of the material itself, the vacuum or the surrounding environment, like the ground, which would make sense considering it is felt in the vertical direction. The 7 Hz signal I presume is originating from the cryocooler as it is felt almost everywhere in the system with a fairly high amplitude and is only present when the cooler is on.

The inside measurements tell us that on the mirror suspension, the most significant frequencies felt are at 8, 10, 35, and 50 Hz and on the base plate, from accelerometer 2 (digital) there are the most significant peaks at 4 Hz and 12 Hz. This however is not confirmed by the analog accelerometer 3, also on the base plate. This accelerometer has peaks at 3, 5 and 25, 60, 80, and 150 Hz.

Moving forward in the future with this project, I would like to retake all the internal cryostat measurements with a consistent time scale and utilizing all the technique to increase the detectors sensitivity levels like decreasing the number of decimal points in the raw data, reading each axis one at a time, and using the maximum baud rate of 2000000. This way we have more easily comparable results. In addition, one could do more tests to figure out where different frequencies were coming from like taking data for a certain location with and without physically shaking or moving different parts of the cryostat to try ad see where each frequency is coming from. Additionally one could look into using higher sensitivity accelerometers as the ones we used in this experiment were cheap and low sensitivity in comparison to others on the market. However, even though these accelerometers were low sensitivity, they did give a decent understanding of what is going on with the cryostat and how it is moving in general.

From these observations, I propose installing damping mechanisms to the base of the frame to minimize vibrations there as that is where it is shaking the most and where the laser is located so we want that location to be as stable as possible. These mechanisms could include installing stabilizing beams to the support legs because we know the support structure is very stable. It could also include frequency isolation foam.

These adjustments will hopefully minimize mechanical noise and help with the future work of the group. In the future the group will be measuring the mechanical loss changes of the material with temperature. These observations will be helpful in these future calculations because they can show how the cryostat is moving and at what frequencies it is vibrating. This will help in terms of figuring out the thermal noise of the cryostat which is a crucial part of mechanical loss measurements.

Appendices

Appendix A: Accelerometer positions

1. Outer positions

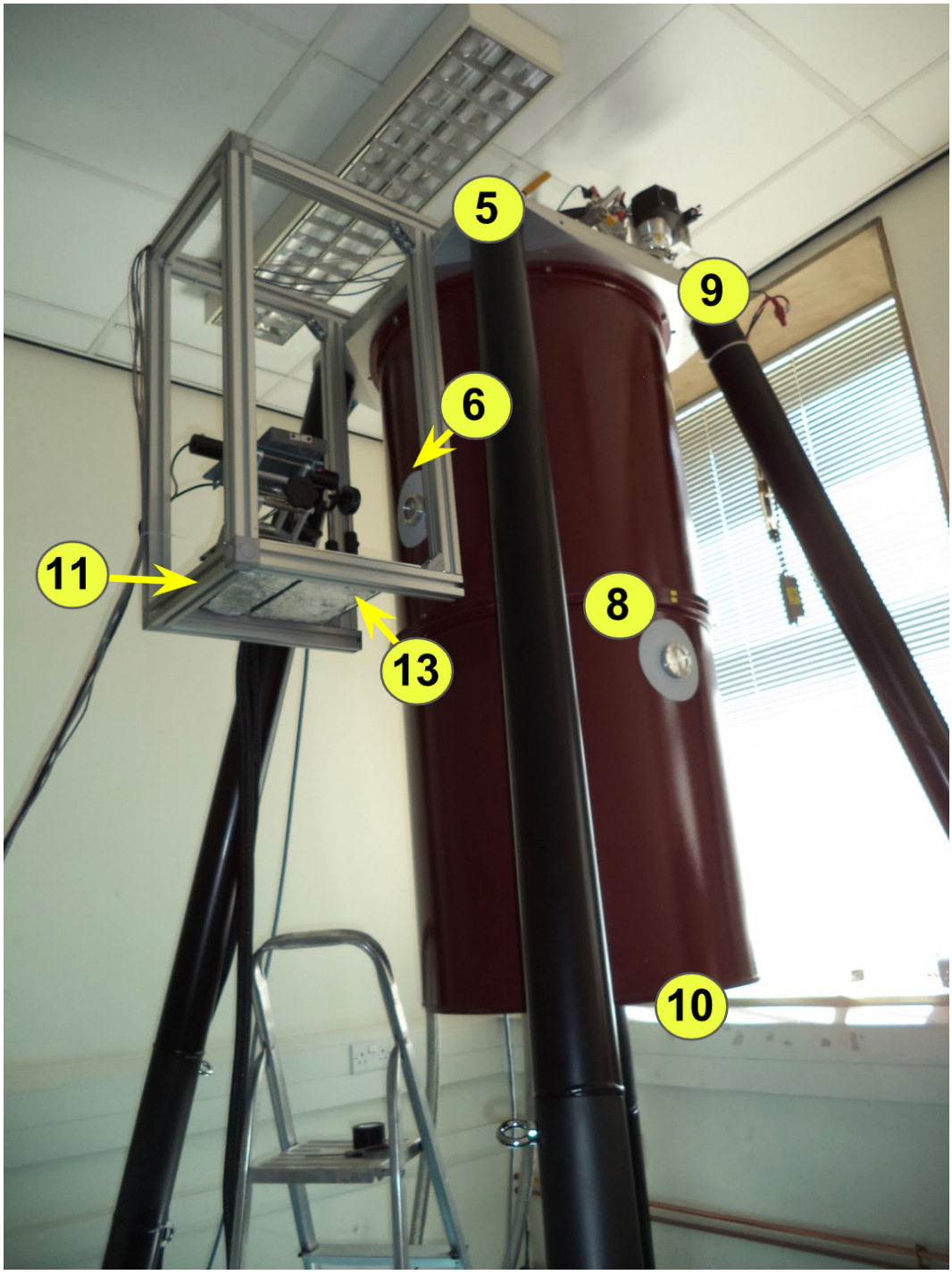

Figure 44: Outer positions for acceleration measurement

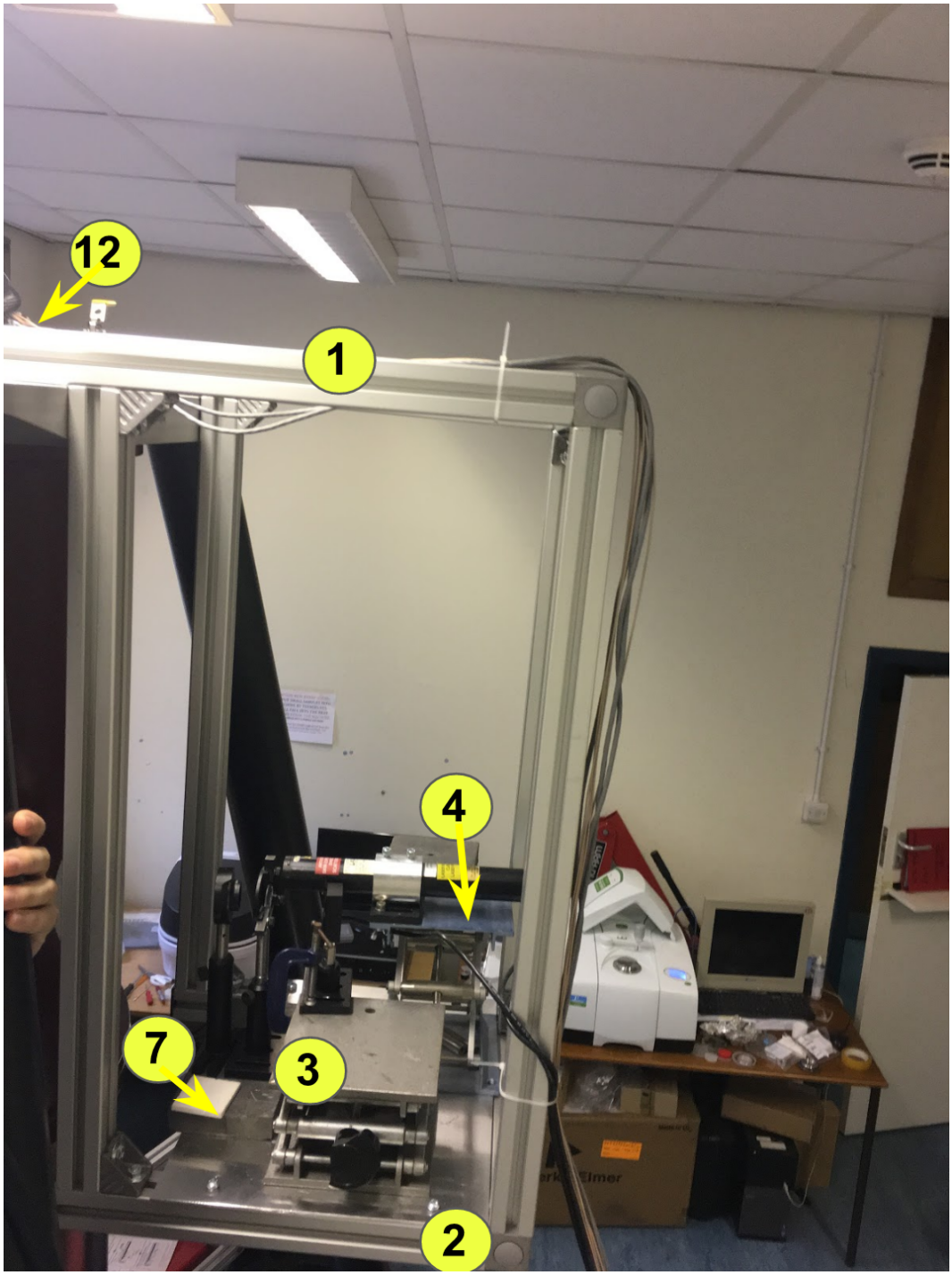

Figure 45: Outer positions for acceleration measurement

2. Inner positions

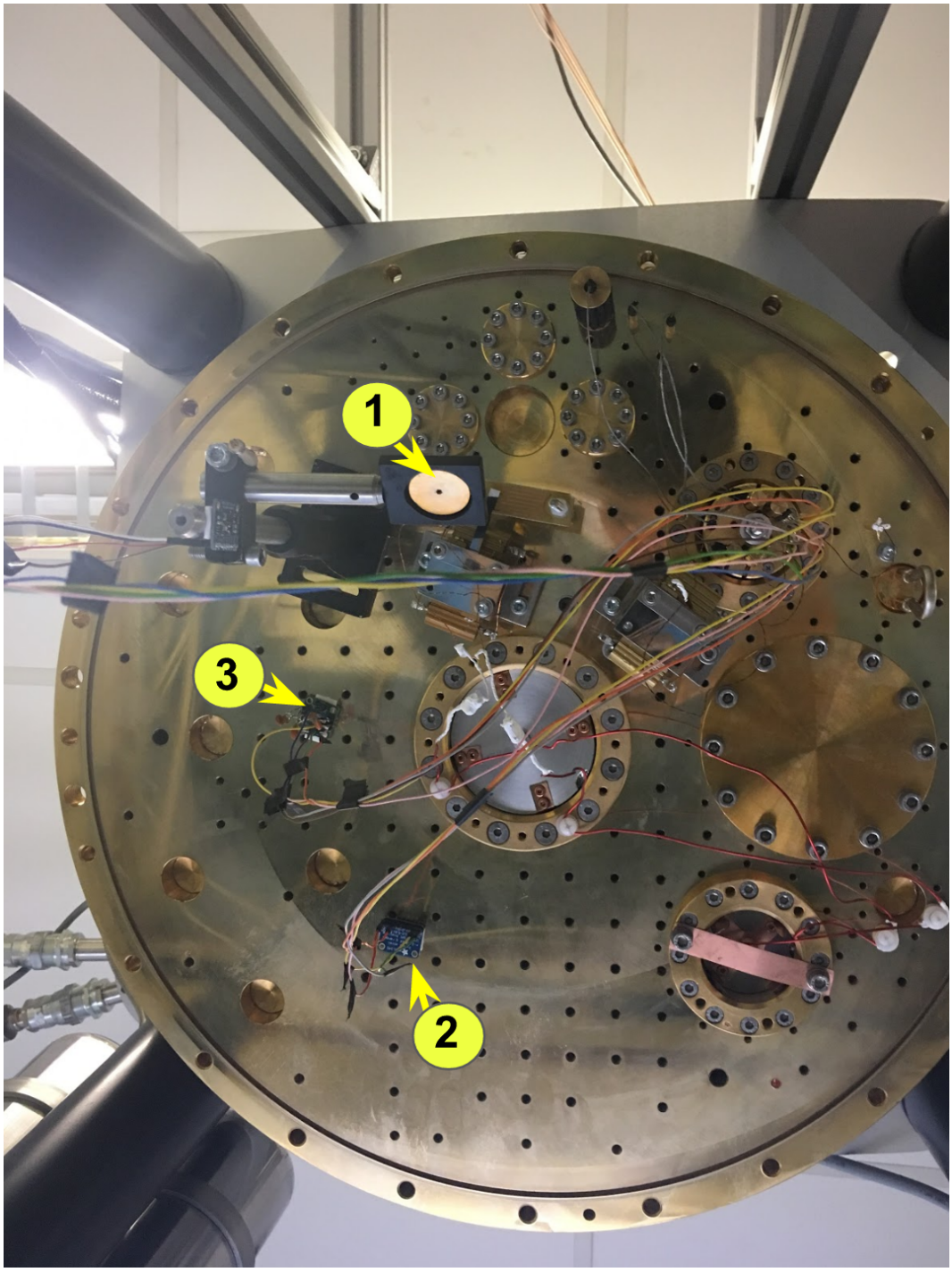

Figure 46: Inner positions for acceleration measurement

Appendix B: Codes

1. Arduino Codes

a. Collecting data from ADXL345

```
  #include <Wire.h>
  #include <Adafruit_Sensor.h>
  #include <Adafruit_ADXL345_U.h>
  // Assign a unique ID to this sensor at the
same time //
  Adafruit_ADXL345_Unified accel =
Adafruit_ADXL345_Unified(12345);
  void setup(void)
  {
  #ifndef ESP8266
  while (!Serial); // for Leonardo/Micro/Zero
  #endif
  //Serial.begin(9600);
  Serial.begin(2000000);
  // Initialise the sensor //
  if(!accel.begin())
  {
  // There was a problem detecting the ADXL345
...  check your connections //
  //Serial.println(‘‘Ooops, no ADXL345 detected
...  Check your wiring!");
  while(1);
  }
  // Set the range //
  accel.setRange(ADXL345_RANGE_16_G);
  }
  void loop(void)
  {
  // Get a new sensor event //
  sensors_event_t event;
  accel.getEvent(&event);
  // Display the results (acceleration is
measured in m/s^2)//
  Serial.print(event.acceleration.x,4);
Serial.print('\n');
  Serial.print(event.acceleration.y,4);
Serial.print('\n');
  Serial.print(event.acceleration.z,4);
Serial.print('\n');
  delay(.1);
  }
```

b. Collecting data from ADXL354

```
  int analogPinx = A0;
  int analogPiny = A1;
  int analogPinz = A2;
  int valx;
  int valy;
  int valz;
  int sensorValuex = 0;
  int sensorValuey = 0;
  int sensorValuez = 0;
  float sensorValuexn = 0;
  float sensorValueyn = 0;
  float sensorValuezn = 0;
  void setup()
  {
  // setup serial
  Serial.begin(9600);
  }
  void loop()
  {
  // read the value from the sensor:
  sensorValuex = analogRead(analogPinx);
  sensorValuey = analogRead(analogPiny);
  sensorValuez = analogRead(analogPinz);
  sensorValuexn=(float)sensorValuex*5/1023/.5*9.8;
  sensorValueyn=(float)sensorValuey*5/1023/.5*9.8;
  sensorValuezn=(float)sensorValuez*5/1023/.5*9.8;
  Serial.println(sensorValuexn,4);
  Serial.println(sensorValueyn,4);
  Serial.println(sensorValuezn,4);
  delay(.1);
  }
```

2. MATLAB Codes

a. Collecting data from ADXL345

```
%% get data

%close open figures
close all

%clear memory
clear all

%open serial port
s2 = serial('COM3');
fopen(s2)
N=1700;
valnum=zeros(3*N,1);

%collect data
flushinput(s2)

tic
for i=1 : 3 * N
      str = fscanf(s2);
      valnum(i)=str2double(str);
end
toc

%collect data
flushinput(s2)

count=0;
```

```
  temp=0;
  for i=1: 3* N
  count=count+1;
        if count==1
              temp=temp+1;
              accelx(temp) =valnum(i);
        end
        if count==2
              accely(temp) = valnum(i);
        end
        if count==3
              accelz(temp) = valnum(i);
              count=0;
        end
  end

  %close serial port
  fclose(s2)

  %record data
  x = accelx;
  y = accely;
  z = accelz;

  fileID = fopen('Calibration test.txt','w');
  fprintf(fileID,'%12s %12s %12s
n','x','y','z');

  for j=1: N-1
        fprintf(fileID,'%12.8f %12.8f %12.8f
n', x(j),y(j),z(j));
  end

  fclose(fileID);

  %% define time domain

  for i=1: N
        t(i)=0.03783* i;
  end

  %% mean

  xmean=x-mean(x)+1;
  ymean=y-mean(y);
  zmean=z-mean(z)-1;

  figure(1)
  plot(t, ymean, 'g-', 'DisplayName', 'Accel
in Y')
  hold on
  plot(t, zmean, 'r-', 'DisplayName', 'Accel
in Z')
  hold on
  plot(t, xmean, 'b-', 'DisplayName', 'Accel
in X')
  hold on
  legend('show')
  xlabel('Time (seconds)')
  ylabel('Acceleration (m/s^2)')
  title('Vibration Test: subracted mean')

  %% polyfit

  x=x-mean(x);
  y=y-mean(y);
  z=z-mean(z);

  coeffx=polyfit(t,x,1);
  coeffy=polyfit(t,y,1);
  coeffz=polyfit(t,z,1);

  corrx=x-(coeffx(1).* t+coeffx(2));
  corry=y-(coeffy(1).* t+coeffy(2));
  corrz=z-(coeffz(1).* t+coeffz(2));

  figure(2)
  plot(t,corrx,'b-','DisplayName','Corrected
X')
  hold on
  plot(t,corry,'g-','DisplayName','Corrected
Y')
  hold on
  plot(t,corrz,'r-','DisplayName','Corrected
Z')
  legend('show')
  xlabel('Time (seconds)')
  ylabel('Acceleration (m/s^2)')
  title('Vibration Test: polyfitted')

  %% standard deviation

  stdx=std(corrx)
  stdy=std(corry)
  stdz=std(corrz)

  %% frequency spectrum FFT

  % Sampling time and frequency

  ts=0.03783;
  fs=1/ts; % Calculate the PSD (power spectral

density) [Pxx,f]=pwelch(corrx,[],[],[],fs);

  [Pxy,f]=pwelch(corry,[],[],[],fs);
  [Pxz,f]=pwelch(corrz,[],[],[],fs);

  % Calculate the ASD asdx=Pxx.^0.5;

  df=f(2)-f(1);
```

```
  rms_asdx=sqrt(sum(Pxx. f))

  asdy=Pxy.∧0.5;
  df=f(2)-f(1);
  rms_asdy=sqrt(sum(Pxy. f))

  asdz=Pxz.∧0.5;
  df=f(2)-f(1);
  rms_asdz=sqrt(sum(Pxz. f)) figure(5)

  loglog(f,asdx,‘b’)
  hold on
  loglog(f,asdy,‘g’)
  hold on
  loglog(f,asdz,‘r’)
  xlabel(‘Frequency (Hz)’)
  ylabel(‘Amplitude ((m/s∧ s)/(sqrt(Hz))’)
  title(‘Vibration Test:     FFT’) %% disconect

serial port delete(s2)
```

b. Collecting data from ADXL345

```
  %% get data %close open figures

  close all %clear memory

  clear all %open serial port

  s2 = serial(‘COM3’);
  fopen(s2)
  N=1700;
  valnum=zeros(3∗N,1); %collect data

  flushinput(s2) tic

  for i=1 : 3 ∗ N
        str = fscanf(s2);
        valnum(i)=str2double(str);
  end
  toc

  %collect data
  flushinput(s2)

  count=0;
  temp=0;
  for i=1: 3∗ N
  count=count+1;
        if count==1
              temp=temp+1;
              accelx(temp) =valnum(i);
        end
        if count==2
              accely(temp) = valnum(i);
        end
        if count==3
              accelz(temp) = valnum(i);
              count=0;
        end
  end

  %close serial port
  fclose(s2)

  %record data
  x = accelx;
  y = accely;
  z = accelz;

  fileID = fopen(‘Calibration test.txt’,‘w’);
  fprintf(fileID,‘%12s %12s %12s
n’,‘x’,‘y’,‘z’);

  for j=1: N-1
        fprintf(fileID,‘%12.8f %12.8f %12.8f
n’, x(j),y(j),z(j));
  end

  fclose(fileID);

  %% define time domain

  for i=1: N
        t(i)=0.03783∗ i;
  end

  %% mean

  xmean=x-mean(x)+1;
  ymean=y-mean(y);
  zmean=z-mean(z)-1;

  figure(1)
  plot(t, ymean, ‘g-’, ‘DisplayName’, ‘Accel
in Y’)
  hold on
  plot(t, zmean, ‘r-’, ‘DisplayName’, ‘Accel
in Z’)
  hold on
  plot(t, xmean, ‘b-’, ‘DisplayName’, ‘Accel
in X’)
  hold on
  legend(‘show’)
  xlabel(‘Time (seconds)’)
  ylabel(‘Acceleration (m/s∧2)’)
  title(‘Vibration Test: subracted mean’)
```

```
  %% polyfit

  x=x-mean(x);
  y=y-mean(y);
  z=z-mean(z);

  coeffx=polyfit(t,x,1);
  coeffy=polyfit(t,y,1);
  coeffz=polyfit(t,z,1);

  corrx=x-(coeffx(1).* t+coeffx(2));
  corry=y-(coeffy(1).* t+coeffy(2));
  corrz=z-(coeffz(1).* t+coeffz(2));

  figure(2)
  plot(t,corrx,'b-','DisplayName','Corrected
X')
  hold on
  plot(t,corry,'g-','DisplayName','Corrected
Y')
  hold on
  plot(t,corrz,'r-','DisplayName','Corrected
Z')
  legend('show')
  xlabel('Time (seconds)')
  ylabel('Acceleration (m/s^2)')
  title('Vibration Test: polyfitted')

  %% standard deviation

  stdx=std(corrx)
  stdy=std(corry)
  stdz=std(corrz)

  %% frequency spectrum FFT

  % Sampling time and frequency

  ts=0.03783;
  fs=1/ts; % Calculate the PSD (power spectral

density) [Pxx,f]=pwelch(corrx,[],[],[],fs);

  [Pxy,f]=pwelch(corry,[],[],[],fs);
  [Pxz,f]=pwelch(corrz,[],[],[],fs);

  % Calculate the ASD asdx=Pxx.^0.5;

  df=f(2)-f(1);
  rms_asdx=sqrt(sum(Pxx. f))

  asdy=Pxy.^0.5;
  df=f(2)-f(1);
  rms_asdy=sqrt(sum(Pxy. f))

  asdz=Pxz.^0.5;
  df=f(2)-f(1);
  rms_asdz=sqrt(sum(Pxz. f)) figure(5)

  loglog(f,asdx,'b')
  hold on
  loglog(f,asdy,'g')
  hold on
  loglog(f,asdz,'r')
  xlabel('Frequency (Hz)')
  ylabel('Amplitude ((m/s^ s)/(sqrt(Hz))')
  title('Vibration Test:     FFT') %% disconect

serial port delete(s2)
```